R-06-107

Effects of grouting, shotcreting and concrete leachates on backfill geochemistry

Miguel Luna, David Arcos, Lara Duro
Enviros, Spain

November 2006

Svensk Kärnbränslehantering AB
Swedish Nuclear Fuel
and Waste Management Co
Box 5864
SE-102 40 Stockholm Sweden
Tel 08-459 84 00
+46 8 459 84 00
Fax 08-661 57 19
+46 8 661 57 19

ISSN 1402-3091
SKB Rapport R-06-107

Effects of grouting, shotcreting and concrete leachates on backfill geochemistry

Miguel Luna, David Arcos, Lara Duro
Enviros, Spain

November 2006

Abstract

The use of concrete to seal open fractures (grouting) and to impermeabilise the deposition tunnels (shotcreting) has been envisaged in the construction of a high level nuclear waste (HLNW) repository according to SKB designs. Nevertheless, the geochemical effect of using concrete in the repository is not fully understood. Concrete degradation due to the interaction with groundwater can affect the performance of other repository barriers, such as the backfill material used for sealing the deposition tunnels. One of the main effects of concrete degradation is the generation of alkaline plumes. For this reason, SKB is currently planning to use a type of concrete whose degradation result in lower pH values than those developed with Ordinary Portland Cement (OPC).

In order to assess the long-term geochemical effect of including low-pH concrete elements in a HLNW repository, we performed a 2D reactive-transport model of a backfilled deposition tunnel that intersects a hydraulic conductive fracture which has been partially grouted. An additional case has been modelled where part of the deposition tunnel walls were covered with a shotcrete layer. The modelling results predict the development of a high-alkalinity plume, larger in the case of considering a grouted fracture, accompanied by the precipitation of CSH-phases in the fracture. However, the effect on the backfill material is only significant if concrete is in contact with the backfill (shotcrete case).

In order to conduct these models, and considering that at the beginning of the present work there was not a specific composition for such a low-pH concrete, its composition has been assumed in order to meet the expected geochemical evolution of concrete degradation according to SKB expectations. This is a pH of pore water of around 11 and the degradation of CSH phases resulting in a source for Ca and Si into the system. For this reason, jennite and tobermorite have been selected, although it is known that jennite is not initially present in concrete, owing that their degradation result in a pH of around 11 and they are a source for Si and Ca into the system.

Contents

1 Introduction 7
1.1 Objectives 8
1.2 Methodology 8

2 Concrete 9
2.1 Concrete components 9
2.1.1 Aggregate 9
2.1.2 Cement 9
2.1.3 Water 9
2.2 Chemical composition of concrete 10

3 Shotcrete and injected grout 13
3.1 Shotcrete 13
3.2 Injected Grout 14

4 Concrete degradation 17
4.1 Hydraulic properties of concrete 17
4.2 Chemical stability of concrete 18
4.2.1 Carbonation 18
4.2.2 Sulphate-induced degradation 18
4.2.3 Chloride-induced degradation: stability of chloride phases 19
4.3 Long-term concrete degradation 19

5 Modelling of the effects of grout on fracture and backfill geochemistry 21
5.1 Conceptual model 21
5.2 Initial and boundary conditions 21
5.2.1 Geometry of the model 22
5.2.2 Materials and hydraulic parameters 23
5.2.3 Boundary conditions 25
5.2.4 Initial conditions 25
5.3 Model results 28
5.3.1 2D simulations considering a layer of shotcrete 28
5.3.2 2D simulations considering a grouted fracture 32

6 Conclusions 39

7 References 41

Appendix A Concrete structure, additives and shotcrete components 45

1 Introduction

Nuclear waste in Sweden is managed by the Swedish Nuclear and Waste Management Co, SKB, which is conducting site investigations for a deep repository in the municipalities of Östhammar and Oskarshamn in the South-East of Sweden. The investigations are conducted in two stages, an initial characterisation phase followed, if the expected site suitability is confirmed, by a complete site investigation. The aim is to build a deep repository at one of these candidate sites if bedrock and other relevant conditions are found suitable. The report presented here will be integrated in the safety report of the SR-Can safety assessment.

Within the SKB's program, the KBS-3 concept is planned to be used as standard design. This concept consists in a multi-barrier system formed by copper canisters stored in vertical holes (KBS-3h is an alternative design where the canisters are planned to be stored horizontally) and surrounded by compacted bentonite. The canisters contain a cast iron insert with the spent nuclear fuel inside. The host rock is granite and the storage depth is expected to be about 500 m. The objective is to completely isolate the spent fuel over the entire assessment period, up to 4,000 years.

The main function of a deep repository for spent nuclear fuel is to avoid the release of radionuclides to the geosphere, ensuring a complete environmental isolation. To this aim, a multi-barrier system in which the host rock (i.e. granite) acts as natural barrier is required.

Low porosities and low hydraulic conductivities characterise granite. In fact, these features make *a priori* to consider this type of rock as a suitable material for waste storage at depth if stable geological areas are considered. However, in these rock formations fractured zones are frequent and even the ideal behaviour of granite could be subjected to some uncertainties. Fractures and fracture zones must be sealed as soon as possible to avoid large groundwater flows at the repository level. The measure taken to reduce groundwater flow is mainly grouting whereas shotcreting mainly is used for securing stability.

Shotcrete is the generic name for cement, sand, and fine aggregate concretes which is applied pneumatically and compacted dynamically under high velocity with the aim of stabilizing and impermeabilise a structure /Hoek 2000/. Injection grout consists of binder and water that after injection will stiffen to a stable hydrated compound in the rock with the objective of sealing open fractures and to reinforce the rock around tunnels and holes in general.

Under repository conditions it is unknown the extent of groundwater affection by the high alkalinity pore water of cement or other components of concrete. In fact, in saturated media it can not be discarded high pH plumes originated by processes of concrete – groundwater interaction. It is unknown whether the increase of pH could affect the isolation capacity of bentonite by changing its swelling capacity or inducing porosity changes due to the precipitation/dissolution of accessory phases in the bentonite pore space.

The reasons presented above highlight the relevance of studying the interaction between groundwater and concrete used in nuclear waste repositories for isolation purposes and the effect induced in other engineered barriers.

1.1 Objectives

The main objective is to assess the effect of hardened shotcrete and injection grout on the geochemical evolution of the backfill material in a deep repository for high level nuclear waste (HLNW). To this aim we present a study of the interaction between groundwater and these structural materials following the sealing of drifts and closure of the repository. The interaction of groundwater and concrete may create hyper-alkaline plumes in the vicinity of the repository whose consequences for the functionality of the barriers are still unknown.

1.2 Methodology

The report is structured into 2 main parts.

The first part of the document aims at presenting the system of concrete, the main processes of degradation and the two different methodologies used for stabilising and impermeabilising the fractures (shotcrete and injected grout). Chapter 2 describes the main composition of concrete, whereas Chapter 3 and 4 describe respectively the techniques of shotcreting and grouting and the most relevant mechanisms of concrete alteration due to its interaction with water. The description is based on an extensive literature review on the composition of cement, shotcrete and concrete likely to be used in the repository construction.

The second part of this document is reported in Chapter 5. In that section we develop a conceptual model of the geochemical evolution of the near-field of the repository system after backfilling and closure of the repository. The model is based on the information presented in previous sections and the information on the geochemical behaviour of bentonite as part of the backfill. This conceptual model is then implemented numerically by using a reactive-transport model simulating a deposition tunnel filled with the backfill material and intersected by a fractured zone. The results of the model are discussed from the perspective of the extent of geochemical alteration of the backfill of a HLNW repository that can eventually result from the hyperalkaline plume generated by the processes of concrete degradation.

In Appendix A, a detailed description of the structure of concrete, its main components and additives is presented.

2 Concrete

Concrete is the base material used in engineering structures. It is basically constituted by a mixture of aggregates, Ordinary Portland Cement (OPC) and water. A detailed description of the structure of concrete and of the several admixtures used to improve its performance in terms of workability and durability can be found in Appendix A to this document.

Concrete obtains its strength capabilities during a hydration process, whose effectiveness depends on environmental variables such as relative humidity and temperature.

2.1 Concrete components

A short description of the role of the different components used in the preparation of concrete (aggregate, cement and water) is presented in this section.

2.1.1 Aggregate

Rock fragments are used as aggregate when preparing the concrete mixture. The main function of aggregates in concrete is to decrease water sorption and provide higher physical resistance. Aggregates must be geochemically inert, in order to avoid alteration of the physico-chemical properties of concrete eventually caused by weathering processes. In some cases, artificial inert aggregates are used.

Although unaltered granite fragments form, in general, excellent aggregates, the presence of some solid phases that can experiment weathering processes, such as sulphates, sulphides and amorphous silica, must be minimised. Amorphous silica (like chalcedony) may react with Portland components producing expansive silicate gels and thus increasing the permeability of concrete; however, this reaction can not take place with low alkali cement or in a low-pH paste as the pH in the pore solution is to low. The oxidation of sulphides may produce acidity, affecting the stability of concrete. Chapter 4 presents a more detailed description of these alteration processes.

2.1.2 Cement

Cement is the main component of concrete. During the hydration of concrete cement acts as paste binder.

It is composed by a mixture of limestone (70–80%) and clay (20–30%), which is heated at approximately 1,450°C, and forms a product known as clinker. Clinker is rapidly cooled down to temperatures of approximately 100°C. Then gypsum ($CaSO_4 \cdot 2H_2O$) or anhydrite are added and the mixture is grinded to a particle size below 100 μm.

Other constituents can be added to the cement paste with the objective of improving the mechanical properties of concrete /Atkins and Glasser 1992/. These additives are described in Appendix A of this report.

2.1.3 Water

The water to binder (w/b) ratio controls the hydration process that provides the mechanical strength to concrete.

In some cases, steel components are used as reinforcing elements. The presence of high chloride concentrations in the water used for the preparation of concrete in this case may enhance the steel corrosion. For this reason, when steel is used for reinforcing, the concentration of chloride in the water must be kept low.

This is especially relevant in shotcrete, given that reinforcing steel fibres are commonly used to prevent eventual fracturing occurring as a consequence of accumulation of tensile stresses (see Appendix A). To prevent steel corrosion some inhibitors could be added, although their use is rare.

2.2 Chemical composition of concrete

The average composition of Ordinary Portland Cement (OPC) is:

- CaO (60–70%),
- SiO_2 (20–25%),
- Al_2O_3 (5–7%),
- Fe_2O_3 (3%),
- SO_3 (3%)
- and some percentages of minor components like Na_2O, K_2O and MgO /Atkins and Glasser 1992/.

Minor differences on the OPC composition are reported in the literature /Engkvist et al. 1996/. Changes in the OPC composition are related to the specific properties expected from the OPC for a given purpose.

In the cement chemistry, the following abbreviations are used:

C: CaO	A: Al_2O_3	F: Fe_2O_3	K: K_2O	M: MgO
S: SiO_2	$\underline{S}$: SO_3	N: Na_2O	H: H_2O	

The main chemical phases of non-hydrated OPC are summarized in Table 2-1.

The process of cement hydration is mainly controlled by w/c or when pozzolanes are used w/b. Porosity, residual water and the hydration kinetics will depend on this ratio, which in general varies from 0.22–0.24 /Atkins and Glasser 1992/ to 0.5 /Taylor 1990/. However, according to Lagerblad (pers. com.), the w/c in an ordinary concrete lies around 0.55 to 0.65, and in concrete used for outdoor infrastructure has w/c between 0.4–0.45; whereas concretes with 0.22 to 0.24 are very rare ultrahigh strength concrete.

During the hydration process, the solid phases listed in Table 2-1 evolve forming mainly: portlandite [$Ca(OH)_2$], ettringite [$Ca_6Al_2(SO_4)_3(OH)_{12}\cdot 26(H_2O)$], monosulphate and different hydrated-calcium-silicates (CSH).

Table 2-1. Chemical phases of Ordinary Portland Cement /Pointeau 2001/.

Phase	Formulation	Mass rate	Impurities
Alite (Tricalcium silicate)	C_3S	50–70%	Al, Mg, Fe
Belite (Dicalcium silicate)	C_2S	15–50%	
Aluminate (Tricalcium aluminate)	C_3A	5–15%	Si, Na, K, Fe
Aluminoferrite (Tetracalcium aluminate ferrite)	C_4AF	5–15%	

The main hydration reactions occurring during the hydration process of Portland cement are /Czernin 1969, in Jolicoeur and Simard 1998/:

$2\ C_3S + 6\ H_2O = C_3S_2 \cdot\ 3\ H_2O + 3\ CH$

$2\ C_2S + 4\ H_2O = C_3S_2 \cdot\ 3\ H_2O + CH$

$C_3A + 6\ H_2O = C_3A \cdot\ 6\ H_2O$

$4\ C_4AF + 2\ Ca\ (OH)_2 + 10\ H_2O = C_3A \cdot\ 6\ H_2O + C_3F \cdot\ 6H_2O$

The chemical composition of the main hydrated phases is summarized in Table 2-2.

The following reactions occurring during hydration were studied by /Czernin 1969, in Jolicoeur et al. 1998/:

$2\ C_3S + 6\ H_2O = C_3S_2 \cdot\ 3\ H_2O + 3\ CH$

$2\ C_2S + 4\ H_2O = C_3S_2 \cdot\ 3\ H_2O + CH$

$C_3A + 6\ H_2O = C_3A \cdot\ 6\ H_2O$

$4\ C_4AF + 2\ Ca\ (OH)_2 + 10\ H_2O = C_3A \cdot\ 6\ H_2O + C_3F \cdot\ 6H_2O$

The hydrated phases are summarized in Table 2-2.

The most abundant components of the cement paste are the CSH phases, whose internal structure is formed during setting and hardening of concrete (see Appendix A). The CSH phases confer a high density to concrete, what determines its final performance. The Ca/Si ratio of the main CSH phases varies between 0.5 and 2.0 (see Table 2-3). The composition of the CSH phases changes over time /Lagerblad et al. 2003/. When it coexists with CH the CaO/SiO_2 ratio is between 1.7 to around 2.2. This is mainly due to incorporation of minute CH. With time CSH phases re-equilibrate, SiO_2-chains polymerize and the CaO/SiO_2 ratio will stabilize around 1.6 to 1.7. A lower ratio demands that the CH is removed with the help of pozzolans in large amounts. This is also the case in old concretes having initial Ca/SiO_2 ratios between 1.6 and 1.7, but decreasing during the leaching process /Lagerblad 2001/.

Of the major reactant phases of cement powder only the thermochemical data for gypsum are essentially complete. However, there is an important lack of reliable thermodynamic data for crystalline calcium silicate hydrates. Some of these cement minerals may dissolve incongruently, which cannot be described through a simple solubility product and requires the development of more elaborate solubility models. Thermodynamic data were selected from /Clodic and Meike 1997, Revertegat et al. 1997/, who used the COM database for these cement phases. These thermodynamic constants are showed in Table 2-3.

Table 2-2. Chemical composition of the main hydrated phases of cement /Atkins and Glasser 1992/.

Phase	Composition
Ettringite (Aft)	$3\ CaO \cdot Al_2O_3 \cdot 3CaSO_4 \cdot 36H_2O$
Monosulfate (AFm)	$3\ CaO \cdot Al_2O_3 \cdot CaSO_4 \cdot 12H_2O$
Hydrogarnet	$3\ CaO \cdot Al_2O_3 \cdot 6H_2O$ – $3CaO \cdot Fe_2O_3 \cdot 6H_2O$
Portlandite (CH)	$Ca(OH)_2$
Hydrotalcite (HT)	$4\ MgO \cdot Al_2O_3 \cdot 10H_2O$
CSH	$(0.9–1.7)\ CaO \cdot SiO_2 \cdot xH_2O$

Table 2-3. Chemical composition of CSH phases, equilibrium constants and molar volumes.

Phase	Ca/Si ratio	Dissolution reaction	Log K (25°C)	Molar volume (cm^3/mol)	Source
Hillebrandite	2.00	$Ca_2SiO_3(OH)_2 \cdot 0.17H_2O + 4\ H^+ = 2\ Ca^{2+} + SiO_2 + 3.17\ H_2O$	36.819	71.79	1
Afwillite	1.50	$Ca_3Si_2O_4(OH)_6 + 6\ H^+ = 3\ Ca^{2+} + 2\ SiO_2 + 6\ H_2O$	60.045	129.23	1
Jennite	1.50	$Ca_9H_2Si_6O_{18}(OH)_8 \cdot 6H_2O$	150	458.35	2
Foshagite	1.33	$Ca_4Si_3O_9(OH)_2 \cdot 0.5H_2O + 8\ H^+ = 4\ Ca^{2+} + 3\ SiO_2 + 5.5\ H_2O$	65.921	154.23	1
Xonotlite	1.00	$Ca_6Si_6O_{17}(OH)_2 + 12\ H^+ = 6\ Ca^{2+} + 6\ SiO_2 + 7\ H_2O$	91.827	264.81	1
Tobermorite	0.83	$Ca_5Si_6O_{16}(OH)_2 + 10\ H^+ = 5\ Ca^{2+} + 6\ SiO_2 + 6\ H_2O$	65.612	286.81	1
Gyrolite	0.67	$Ca_2Si_3O_7(OH)_2 \cdot 1.5H_2O + 4\ H^+ = 2\ Ca^{2+} + 3\ SiO_2 + 4.5\ H_2O$	22.910	136.85	1
Okenite	0.50	$CaSi_2O_4(OH)_2 \cdot H_2O + 2\ H^+ = Ca^{2+} + 2\ SiO_2 + 3\ H_2O$	10.382	94.77	1

1. /Clodic and Meike 1997/
2. /Revertegat et al. 1997/.

It is worth noting that during hydration, coupled cationic substitution processes are common in ettringite they are very limited in CSH phases. Si, for example, may be exchanged by Al and Fe.

Although portlandite [$Ca(OH)_2$] is the most important concrete-forming mineral during early stages of cement hydration, other phases, such as singenite [$K_2Ca(SO_4)_2 \cdot H_2O$] or brucite [$Mg(OH)_2$] are also formed.

3 Shotcrete and injected grout

Grout will be injected in the rock to seal individual fractures and/or fractured zones. The sealing of any highly fractured zones will also prevent instability caused by erosion of rock material.

Grout and shotcrete use finer components than standard concrete, as additives or additions (see Appendix A). Additives modify some properties of grout and shotcrete, such as workability (e.g. superplastizisers). Additions are powdered materials added to the mixtures of cement to improve its consistency in the short term (i.e. silica fume) or its mechanical resistance (i.e. addition of steel fibres to shotcrete). As a consequence the use of these components will modify hydraulic properties of the final material.

3.1 Shotcrete

Shotcrete is the generic name for the mixture of cement, sand, and fine aggregate concrete that is applied pneumatically and compacted dynamically under high velocity with the aim of stabilizing and impermeabilizing an engineering structure /Hoek 2000/.

The most common additives of shotcrete are superplasticizers. These compounds are organic polymers that enhance the workability of concrete by keeping a low w/c ratio.

Other admixtures, like fly ash or silica fume, are considered additions and they are used to improve the mechanical resistance of concrete, to increase the viscosity to make a better pumpability and to improve the cohesion to lower the rebound when shot. These pozzolanic components have a very low grain size, large specific surface area and, consequently, accelerate the setting of concrete if added during the hydration process.

Shotcrete can be applied in two different ways /Hoek 2000/: i) dry-mix and ii) wet-mix, which are briefly described below.

i) Dry-mix process (Figure 3-1): The dry shotcrete components, which may be slightly pre-damped to reduce dust, are fed into a hopper with continuous agitation. Compressed air is introduced through a rotating barrel or feed bowl to convey the materials in a continuous stream through the delivery hose. Then, water is added to the mix at the nozzle. However, a set accelerator is not always needed. Instead other tricks are used like using cement without gypsum to give a false setting so that the shotcrete stays in place.

ii) Wet mix process (Figure 3-2): In this case, a set accelerator is added at the nozzle where air is added to project the material onto the rock surface.

The addition of a set accelerator makes the concrete stiff enough to stay at the walls /Lagerblad et al. 2003/. There are different types of set accelerator. It used to be waterglas (alkali silicate) but today a type called alkalifree set accelerator is used. It is mainly based on aluminium sulphate and it forms ettringite in contact with pore solution.

The thickness of a shotcrete layer normally ranges between 30 and 70 mm. The shotcrete used for the repository is assumed to contain steel fibres.

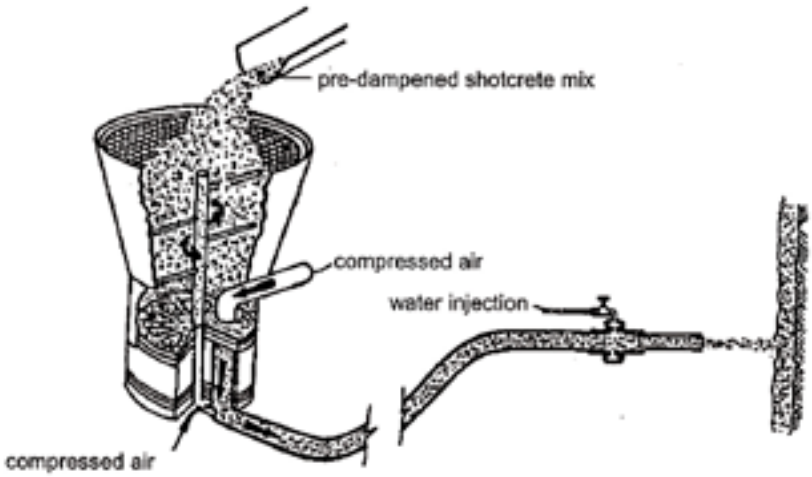

Figure 3-1. *Simplified sketch of a dry mix shotcrete system /Hoek 2000/.*

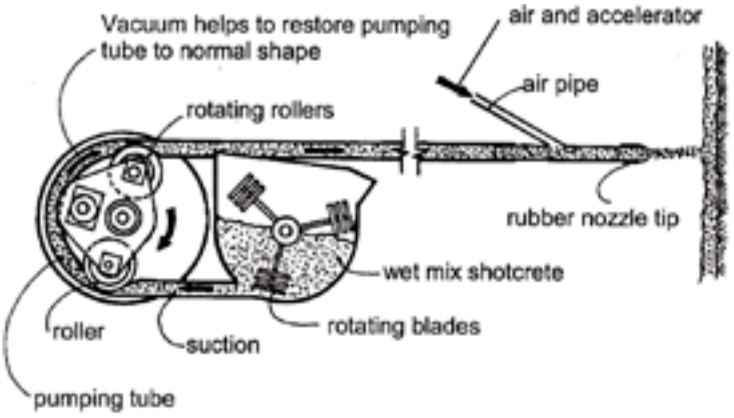

Figure 3-2. *Typical wet mix shotcrete machine /Hoek 2000/.*

Due to the excavation conditions expected during the building of the repository, shotcrete will be probably applied by wet-mix process.

The composition of shotcrete is summarized in Table 3-1 and Table 3-2.

3.2 Injected Grout

The bases of injected grout application are similar to those of shotcrete. The main difference is that grout is injected in open fractures to avoid both the lowering of the groundwater table and the up-coming of deep salt water.

Grouting will be applied to seal open fractures and to anchor the rock bolts used to tie unstable or potentially unstable rock structures, reinforcing the rock around the tunnels.

Fractures and fractured zones need to be grouted to avoid or to decrease the water inflow into the tunnel. The smaller fractures in the deposition tunnel (aperture approx < 0.1 mm) will most likely be grouted with mainly silica sol, while larger fractures will be grouted with cement-based grout of low pH. The final receipt for the grout based on low pH is presently not available but the most composition most likely to be used corresponds to a mixture of Portland cement (Ultrafin 16) and Grout Aid, and Silica Sol for very thin fractures. The composition of these grout materials is summarized in Table 3-1.

The rock sections that need to be grouted are identified prior to the excavation of the tunnel. Grouting holes are then drilled and grout is injected prior to the excavation of the tunnel.

Grout may be used to anchor rock bolts made of steel. Rock bolts for normal conditions may be around 1.6–4.2 m long and 25 mm in diameter while the boreholes drilled in the rock walls normally are around 50 mm in diameter. The anchoring grout is also of low pH. The low alkali paste and the mortar grout for rock bolts are summarized in Table 3-2.

Table 3-1. Chemical composition of low pH grout materials /SKB 2004/.

Type	Product name Ultrafin 16 Sulphate resistant Portland cement	Silica sol Colloidal silica	Grout aid Silica Slurry, Aqueous solution
CaO	64.8		–
SiO_2	22.3	100	86
Al_2O_3	3.4		–
Fe_2O_3	4.3		–
SO_3	2.4		–
Na_2O	–		–
Others	2.8		C < 2.5

Table 3-2. Recipes – low alkali grout for rock bolts and grouting (density of 1,328 kg/m). Reference: Cement recipe P3A, used in pilot test at ONKALO /Sievänen et al. 2005/.

Component	Amout (kg) Anchoring grout for rock bolts	Grout	Shotcrete	Comment
Water	696	599	214	
Cement	–	–	306	Ordinary Portland Cement
Ultrafin 16	–	299		Micro cement. Sulphate resistant Portland Cement.
				Density: 800–1,500 kg/m^3
				Composition is given in Table 3-1
White cement	596	–	–	Low alkali Portland Cement (Aalborg)
				Density: 1,100 kg/m^3
				Composition is given in Table 3-1
Grout Aid	–	419	–	Dispersed silica fume, (50 wt% SiO_2, 50 wt% water)
				Density: 1,350–1,410 kg/m^3
Silica Fume	255		204	Dispersed silica fume, (50 wt% SiO_2, 50 wt% water) density 1,350–1,410 kg/m^3;
SP 40	2	11	7	Superplastiziser, density 1,260 kg/m^3; sulfonate melamin-polykondensat
Ballast	–	–	1,500	
Fibres	–	–	70	Steel fibres
Density	1,549	1,328	2,301	
Vct vinyl addition polymer			214	

4 Concrete degradation

4.1 Hydraulic properties of concrete

The hydrodynamic properties of concrete, and especially its hydraulic conductivity, control the penetration of water into the material. When concrete is exposed to a pressure gradient (head of water), permeability becomes relevant and obeys Darcy's flow, assuming laminar flow. In fact, only small humidity differences between the two concrete boundaries can produce the movement of water. Considering the extremely low permeability of concrete, and considering that shotcrete is even less permeable due to its physical characteristics, it is expected that diffusion will be a relevant transport process through it.

Concrete permeability depends on the size, distribution and connectivity of its pores. This, in turn, is dependent on the w/c ratio of concrete and the degree of hydration of the cement paste. The existing relationships between porosity, permeability and w/c ratio were studied by /Neville 1981, Oliver and Massat 1992/; extracted from /Lagerblad and Trägard 1994, p.30/. From these studies it was stated that concrete permeability ranges from 10^{-14} to 10^{-10} m/s depending on the w/c ratio and maturity, which influence the pore structure (Table 4-1). At a w/c ratio of 0.5 the hardened cement has a porosity of about 30% by volume.

The cement paste is formed by crystalline phases (portlandite, monosulphate, ettringite) and gel phases (CSH). The porosity is divided into larger capillary pores (diameter about 1,000 nm), as a consequence of using large w/c ratios, and smaller gel pores (about 150 nm). Water can flow more easily through the capillary pores and, therefore, cement pastes (capillary + gel pores) are up to 100 times more permeable than cement, which only contains gel pores (i.e. cements of low w/c ratio).

Concrete hydration processes will induce changes in the porosity and hydraulic conductivity with time. The initial values of hydraulic conductivity can be reduced down to two orders of magnitude in about one year /Neville 1981/.

Table 4-1. Hydraulic conductivities of concrete for several w/c ratios and temperatures /Lagerblad and Trägardh 1994; Table 6-1, p. 30/.

/Tang and Nilsson 1993/				/Neville 1981/ (20°C)		
w/c	T (°C)	K (m/s)	Age	w/c	K(m/s)	Age
0.30	20	10^{-14}	28d	0.38	$2.5 \cdot 10^{-15}$	> 1 yr
0.40	20	$2 \cdot 10^{-14}$	28d	0.42	$8.2 \cdot 10^{-15}$	> 1 yr
0.50	20	$3 \cdot 10^{-14}$	28d	0.48	$2.4 \cdot 10^{-14}$	> 1 yr
0.60	20	$2.3 \cdot 10^{-13}$	28d	0.66	$5.8 \cdot 10^{-13}$	> 1 yr
0.70	20	$2.2 \cdot 10^{-13}$	28d	0.70	10^{-13}	> 1yr
0.70	20	$1.4 \cdot 10^{-13}$	> 1yr	0.71	$1.5 \cdot 10^{-11}$	> 1yr
0.40	27	$7 \cdot 10^{-14}$	28d			
0.40	60	$5.3 \cdot 10^{-13}$	28d			

4.2 Chemical stability of concrete

Portland cement-based concrete can experiment degradation processes due to water-solid interaction reactions. These reactions are governed by the principles of thermodynamics and kinetics. The exact definition of these processes is complex, given the lack of definition of some of the individual phases present in concrete /Lagerblad and Trägardh 1994/. In this section, the main processes responsible for concrete degradation are described: carbonation (carbon dioxide attack), sulphate-induced and chloride-induced degradation.

4.2.1 Carbonation

Carbonation occurs when carbon dioxide from the atmosphere dissolves in the pore solution of cement paste, producing CO_3^{2-}, which reacts with Ca^{2+} to produce $CaCO_3$ (calcite). This chemical process may occur before the process of sealing of the repository tunnels, given that the shotcrete layers are exposed to atmospheric conditions during this period. Due to human activities and the various engines being used, air in tunnels may be enriched in carbon dioxide, what will favour the carbonation process.

Carbonation consumes portlandite [$Ca(OH)_2$], according to the following reaction:

$Ca(OH)_2 + CO_2 = CaCO_3 + H_2O$

After $Ca(OH)_2$ depletion, the CSH gels are decalcified and decomposed. The Afm and Aft phases (monosulphate and ettringite, respectively) react to form carbonate phases. The end-products of the complete carbonation are calcite, amorphous silica, hydrocarboaluminates and various Al- and Fe-hydroxides.

During the first step, the consumption of $Ca(OH)_2$ causes a decrease in pH to values close to 12.4. Then the CSH gels will change in composition. The next step will be when monosulphate decompose (leading to a pH of 11.6) and later ettringite (pH = 10.5). It normally goes down to around 8–9 when buffered by calcite /Lagerblad and Trägard 1994/.

The accessibility of the air to pore water controls the rate of carbonation of concrete. Thus, parameters such as open porosity, permeability, w/c ratio and relative humidity exert an important control of the carbonation rate. The rate of carbonation is mainly determined by the humidity in the capillary pores /Lagerblad 2005/. When the cement paste is dry the $CO_2(g)$ can penetrate deep in the capillary system and the rate of carbonation will be fast. When humid the transfer is mainly diffusion controlled in the water filled capillary pores and is very much slower.

Low inorganic carbon concentrations can also alter the cement paste, given that CO_3^{2-} can substitute SO_4^{2-} in some of the hydration phases /Lagerblad and Trägard 1994/. An example of this process is found in the formation of thaumasite. It is found in carbonated cement paste and it formed in normal cement paste due to sulphate reactions. This, however, needs carbonate aggregates and is a form of sulphate attack. Thaumansite belongs to the same family as ettringite but it only form at temperatures below around 18°C. The formation of thaumasite in cements, mortars and concretes has been recently studied by /Bensted 1999/.

4.2.2 Sulphate-induced degradation

The OPC contains a few % of calcium sulphates (gypsum) which controls the setting time during the hydration of concrete. Sulphate can form monosulphate (AFm) and ettringite (Aft).

As mentioned in Chapter 2, ettringite is one of the main minerals formed in concrete during the first stages of cement hydration. When concrete pore water is depleted in sulphate, the early ettringite reacts with the remaining aluminate and forms monosulphate.

Ettringite is destabilized under very low sulphate concentration /Engkvist et al. 1996/. Under high sulphate concentrations the formation of ettringite is enhanced and, eventually, also gypsum can precipitate. The formation of both ettringite and gypsum is associated to a volume increase that can, eventually lead to fracturation processes. Ettringite requires aluminium to

form, thus in sulphate-rich environments, the content of aluminium in concrete must be kept low /Lagerblad 1999/.

The stability of ettringite was investigated by /Damidot et al. 1992/. The stability of both ettringite and monosulphate is pH controlled. Potentiometric measurements indicated disappearance of ettringite and monosulphate at pH below 10.7 and 11.6, respectively. At lower pH values, only gypsum and aluminium sulphate remain.

The stability of ettringite and monosulphate is, however, also dependant on the alkali content and on temperature:

$3CaO{\cdot}Al_2O_3{\cdot}6H_2O+2Ca(OH)_2+CaSO_4{\cdot}2H_2O+2(K,Na)_2SO_4+76H_2O =$

$= 3CaO{\cdot}Al_2O_3{\cdot}3CaSO_4{\cdot}32H_2O+4(K,Na)OH$

At low temperatures (20°C) ettringite is the stable phase, whereas for temperatures above 60°C the reaction reverses to the left and at very high temperatures syngenite can precipitate. Results on thermal treatment of concrete indicate that for temperatures above 70 to 80°C ettringite becomes unstable /Brown and Bothe 1993/.

4.2.3 Chloride-induced degradation: stability of chloride phases

Normal cements have very low chloride content. Excess in chloride may produce corrosion of the reinforcement elements and cause a volume expansion within the concrete leading to micro-fracturing.

Chloride from the pore solution enters the CSH gel and binds to the AFm phase. The diffusion of chloride into concrete depends on both the w/c ratio and the cement type /Page et al. 1981/. From several experimental diffusion tests run by using seawater, diffusion coefficients of chloride in a concrete with Degerhamn Standard Portland Cement of 2.7, 4.2 and $4.8{\cdot}10^{-12}$ m^2/s at w/c ratios of 0.35, 0.40 and 0.50, respectively were determined /Lagerblad and Trägard 1994/. These authors also observed a decrease in the diffusion coefficient with the aluminate content.

The main AFm phase (monosulphate) has the formula $3CaO{\cdot}Al_2O_3{\cdot}CaSO_4{\cdot}12H_2O$, the replacement of sulphate by chloride, lead to the formation of the Friedel's salt. Only a little number of studies about the behaviour of chloride in cements have been carried out and chloride diffusion in cements is not a well understood process yet.

Temperature and chloride concentration control the chemical reactions involved in chloride attack. It is known that for temperatures above 40°C and chloride concentrations above 10,000 mg/L ettringite can decompose to form Friedel's salt and gypsum (below 20°C trichloride forms instead). These conditions are expected in the repository and should be carefully evaluated to assess the relevance of this type of concrete degradation.

4.3 Long-term concrete degradation

The stability of hydration products in hardened cement paste depends on the chemical composition of the pore solution. As a consequence, the interaction with aqueous environments does not result in a continuous alteration over distance but in the formation of a zonation pattern, where regions with different solid compositions show relatively sharp transitions between them. At a fixed point different degradation processes follow one each other due to the fact that the reactive front moves with time. These processes include dissolution of cementitious phases, transport of dissolved chemical species and re-precipitation of secondary minerals /Pointeau 2001/.

The observed textural relationships indicate that chemical attack is triggered by permeable heterogeneities which serve as pathways for the percolating water. In all investigated tunnel structures with shotcrete in contact with groundwater the long-term processes of leaching and the formation of sulphate minerals, predominantly thaumasite, have been detected along

internal pathways and along the interface of the lining. As a consequence thaumasite may be a very common finding in a large number of underground constructions /Lagerblad and Trägardh 1994/.

The equilibrium pore water in concrete is hyper-alkaline, with pH values around 13. Nevertheless, depending on the concrete characteristics some slight variations could be assumed. pH values can be used to monitor concrete degradation /Delagrave et al. 1994/. Concrete quality depends then, not only on concrete composition, but also on the environmental conditions.

The initial pH of the pore solution is maintained at around 13, but when an external fluid comes into contact with concrete phases this value will start to decrease lower values. Modelling exercises conducted by /Atkinson 1985, Pointeau 2001/ allowed the differentiation of five pH-evolution stages in concrete pore water (see Figure 4-1).

1) **Phase I:** corresponding to fresh cement. Pore water has pH values over 12.5, high ionic strength and high K^+ and Na^+ concentrations. These features are the result of the dissolution of alkali hydroxides. The duration of this phase depends on the water flow through cement. /Atkinson 1985/ estimated the duration of this phase in approximately 10,000 years by assuming a flow rate of 10^{-10} m/s.
2) **Phase II:** Soluble salts of Na^+ and K^+ have been completely dissolved and major phases are CSH and portlandite. The dissolution of portlandite buffers the pH to values around 12.4.
3) **Phase III:** Portlandite has been completely dissolved and the CSH phases control the chemical evolution of the system. pH decreases from 12.4 to 10, and also the ionic strength decreases. In this stage the Ca/Si ratio decreases from 1.7 to 0.85.
4) **Phase IV:** Ca/Si ratio of CSH phases decrease in this stage to 0.83 buffering the pH at a value of 10. At this stage the uptake of Mg has to be also considered /Lagerblad 2001/.
5) **Phase V:** Concrete has been completely altered and the pH of the pore solution will be determined by the pH of the infiltration water and by calcite as the final alteration product.

Summarizing, the CSH phases constitute the last protective barrier against concrete degradation. Once the CSH completely degrade, the major solid phases controlling the chemistry of the system will be calcite and silica gel.

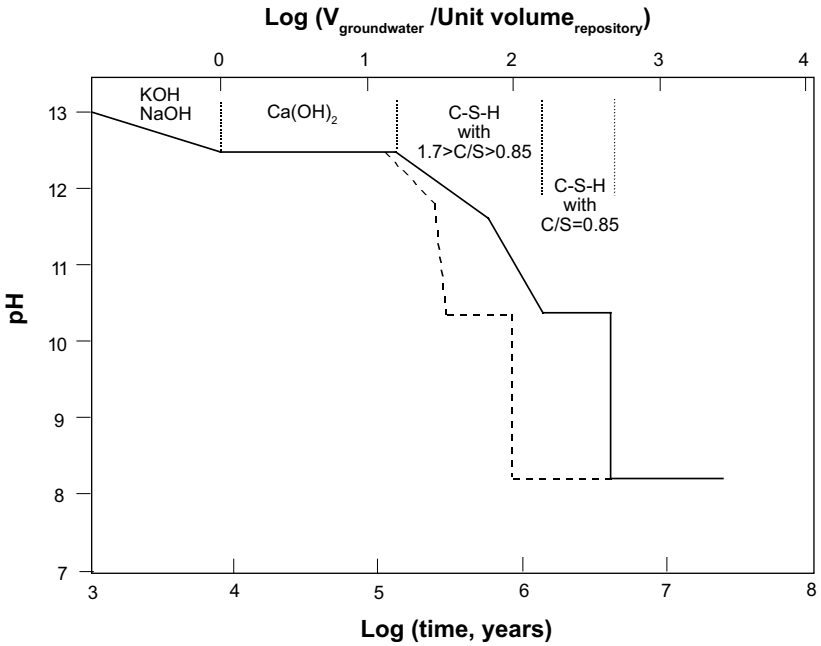

Figure 4-1. *Evolution of pH as a function of degradation of the hydrated phases of cement. Results obtained by modelling tests /Atkinson 1985/.*

5 Modelling of the effects of grout on fracture and backfill geochemistry

The use of highly alkaline structural materials such as concrete in a repository for radioactive waste may produce high pH (hyper-alkaline) plumes due to interaction with groundwater. The effects that these high alkaline plumes could have on the material used as a backfill in the deposition tunnels of a HLNW repository are uncertain and consequently they need to be further evaluated.

A coupled 2D reactive-transport model that simulates a deposition tunnel in a deep geological HLNW repository has been developed. The objective of this model is to assess the effect of the eventual development of a hyperalkaline plume in the vicinity of the repository due to the interaction of groundwater with the cementitious materials used in grouting and shotcreting. The work is focused on the effect of the hyperalkaline plume on the material used to backfill the tunnels after the closure of the repository.

5.1 Conceptual model

Groundwater is assumed to flow through fractures in the granitic host-rock. Some of these fractures may be intersected by the excavated galleries of the repository, allowing groundwater to flow to the tunnels.

Shotcreting is one of the techniques used to avoid the intrusion of groundwater into the tunnel. This technique consists in the impermeabilization of the tunnel walls by using concrete.

Grouting is a technique used to stabilise mechanically the system. It is based on the application of concrete to the main conductive fractures intersected by the excavated galleries.

After the operational stage of the repository, the tunnels will be backfilled by using either bentonite or a mixture of bentonite and crushed rock in a 30/70 ratio.

These techniques, though, cannot guarantee a complete impermeabilisation of the fractures, remaining some parts of them still open to groundwater circulation during the operational stage. Thus, groundwater can interact with concrete first in the grouting or in the shotcrete and then with the backfill, leading to the alteration of the geochemical state of the backfill.

The effect of a high pH plume into both the granite host rock (in the conductive fractures) and the backfill can lead to the precipitation of CSH-phases in these parts of the system. However, this pH plume can also be buffered to lower values due to the precipitation of calcite (enhanced by the increase in calcium concentration due to the dissolution of CSH-phases).

The precipitation/dissolution of other minerals in the different zones (as gypsum, amorphous silica and Fe-bearing phases), as well as the cation exchange and surface acidity reactions in the clay fraction of the backfill, can also contribute to buffer pH at lower values.

5.2 Initial and boundary conditions

According to this conceptualisation, groundwater is assumed to interact with the 30/70 crushed granite/MX-80 bentonite-backfill. The section in Figure 5-1 reproduces a fracture plane that intersects the tunnel orthogonally to its axial plane. This fracture is hydraulically very conductive and simulates a continuous water supply into the tunnel. As the repository will be located at a depth of around 500 m, a regional flux of groundwater in the horizontal direction is considered.

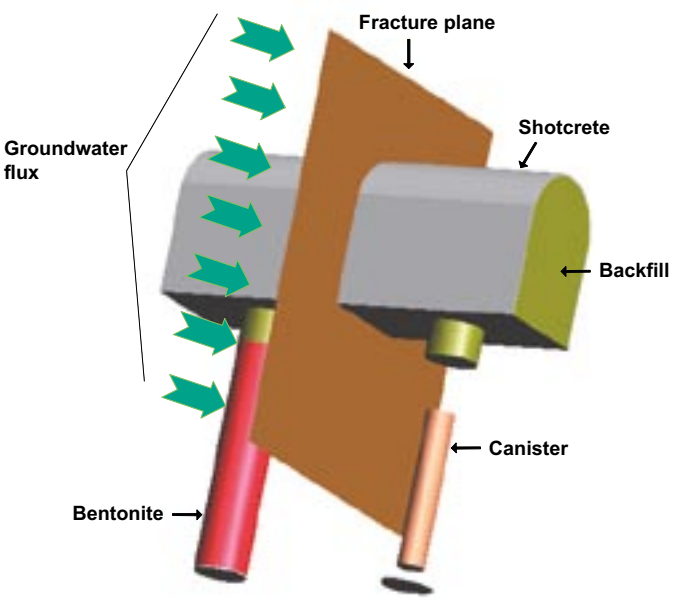

Figure 5-1. *Configuration of the SKB concept for spent fuel storage at depth, showing a hypothetical fracture intersecting the deposition tunnel. A layer of shotcrete applied on the inner part of the excavation has also been considered.*

Initially, the simulation time was thought to be 50,000 years, considering as the initial time immediately after the saturation of the backfill. However, as most changes were predicted to occur during the first thousands of years, a total simulation time of 4,000 years will be considered.

Numerical calculations have been done by using the code PHAST /Parkhurst et al. 2000/. This code is the result of coupling a transport code, HST3D /Kipp 1997/ and a geochemical code, PHREEQC /Parkhurst and Appelo 1999/. The reaction-transport equations are solved by sequential approach in which solute transport and chemical reaction are divided into separate calculations for each time step. First, the components are transported and then geochemical reactions are calculated. PHAST uses porous media properties and boundary conditions defined by zones for a point-distributed-finite-difference grid.

5.2.1 Geometry of the model

The model uses a structural mesh in 2D of about 10,122 square elements covering a squared domain of 80·40 m. This area represents the fracture plane with the exception of the deposition tunnel, which is centred on the Z-axis and on the 20 m coordinate of the X-axis, and considered as a square of 6 m side length (Figure 5-2). Three different configurations have been considered:

- The first configuration of the conceptual model considers a layer of 0.1m thickness, located on the inner tunnel boundary and simulating the shotcrete only on the walls and ceiling respectively (Figure 5-2a).
- The second configuration considers that the fracture plane has been grouted in almost all its extension, to impede groundwater entering into the deposition tunnel (Figure 5-2b).
- The third configuration considers a tunnel only filled by a mixture of crushed granite-bentonite (MX-80 type) without any additional structural material. This configuration represents what would happen to the backfill in case of no grouting or shotcreting.

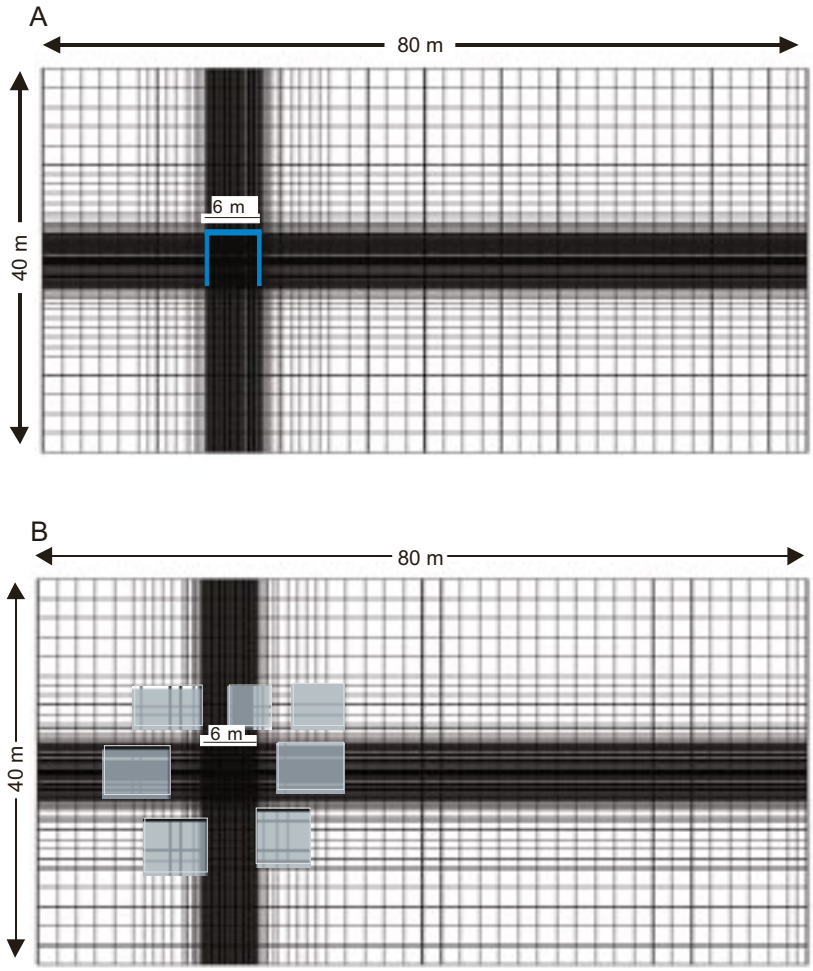

Fi *'crete layer applied on the tunnel walls and roof, whereas in (B) grouting is simulated by several patches in the same plane of the fracture.*

The mesh element distribution has been selected to allow a better numerical resolution around and within the tunnel, where higher hydraulic gradients are expected for the numerical solution. Spatial Δx and Δy vary progressively from 2 m at the domain boundaries to 0.1 m in the surrounding of the deposition tunnel.

5.2.2 Materials and hydraulic parameters

The model presented here consists on three media: (1) fracture, (2) backfill and (3) shotcrete or grout, depending on the configuration considered in simulations. The geometry of the model, the material distribution and the hydrological parameters considered for each material will determine its hydrodynamic behaviour and consequently the hydrodynamic response during simulations.

It has been assumed a saturated media and stationary flux; therefore, the water flux will depend only on hydraulic conductivity and porosity if the hydraulic gradient is fixed. The ground-water flow equation used in PHAST is given in /Kipp 1997/. The dependent variable internal to the simulator is pressure; however, given the assumptions of PHAST, equivalent equations can be written by using potentiometric head as the dependent variable (Equation 5.1).

$$Ss\frac{\partial h}{\partial t} = \nabla(K\nabla h) + r \qquad \text{Equation 5.1}$$

with $h = \frac{p}{\rho g} + z$

where *Ss* is the specific storage (per meter, m^{-1}); *h* is the potentiometric head (m); *t* is time (s); *K* is the hydraulic conductivity tensor (m s^{-1}); *r* is the source flow rate intensity (m^3 m^{-1} m^{-3}); *p* is the pressure (Pa); ρ is the water density (kg m^{-3}); *g* is the gravitational acceleration (m s^{-2}) and *z* is the elevation coordinate.

It is worth to notice that non-transient flux will be considered in the calculations, that is, the potentiometric head will not change in time during calculations and therefore the differential term ($\partial h/\partial t$) is equal to zero. The storage capacity (S_S) is also neglected because it depends on the potentiometric head variation, considered constant. The source flow rate intensity (r) or recharge term is equal to zero. The general equation of water flux (solved by PHAST) is therefore simplified, neglecting these hydrogeological terms.

Darcy law in Equation 5.1 implicitly carries the Darcy velocity in porous media (see Equations 5.2 and 5.3):

$$q = -K\nabla h \qquad \text{Equation 5.2}$$

$$v = \frac{q}{\phi} \qquad \text{Equation 5.3}$$

where φ is porosity; *q* is Darcy flux; *K* is the hydraulic conductivity and *v* is the Darcy velocity component.

No information about hydraulic conductivities of rock and transmissivity of fractures is available, thus we will assume that the results obtained by /Hartley et al. 2004/ at Forsmark site are applicable. According to the experiments carried out at Forsmark, for a depth interval between 300 and 500 m below the ground surface, hydraulic conductivities in the rock range from 10^{-6} to 10^{-7} m·s^{-1}. Some values of intrinsic permeability (k_i) of fractures at the same depth interval have also been reported by /Hartley et al. 2004/, being the reference value around 10^{-15} m^2. The hydraulic conductivity (*K*) is calculated by means of Equation 5.4:

$$K = \frac{g\rho}{\mu} k_i \qquad \text{Equation 5.4}$$

where *g* is gravity; ρ is density and μ is viscosity.

Water viscosity is $2.1\cdot10^{-6}$ kg $m^{-1}s^{-1}$ and the estimated hydraulic conductivity (K) in the fractures is of in $5\cdot10^{-7}$ m·s^{-1} (Equation 5.4).

By considering a fracture zone with a thickness of 0.4 m a transmissivity of $2\cdot10^{-7}$ m^2·s^{-1} is obtained.

A porosity for the fracture zone of 20% is considered, in agreement with /Dershowitz et al. 2003/.

Information related to the hydraulic behaviour of concrete has been obtained from the SFR repository /Holmén and Stigsson 2001/. According to these authors the hydraulic conductivity of concrete used in SFR range from 10^{-11} to $8.3\cdot10^{-9}$ m·s^{-1}, although we selected a value of $8.3\cdot10^{-10}$ m·s^{-1}, which is the hydraulic conductivity assigned to the concrete layer in the SFR repository by /Holmén and Stigsson 2001/.

Porosity values and effective diffusion coefficients range from 0.1 to 0.31 and from 10^{-11} to 10^{-10} $m^2 \cdot s^{-1}$, respectively, depending on w/c ratios /Höglund 2001, Pereira and Sundström 2004/. We selected a porosity value of 0.3 and a value for effective diffusion coefficient of 10^{-10} $m^2 \cdot s^{-1}$.

According to /SKB 2006/ the porosity in the 30/70 backfill is 36.3% and the hydraulic conductivity is $5 \cdot 10^{-11}$ $m \cdot s^{-1}$. The effective diffusion coefficient has been considered $1.2 \cdot 10^{-10}$ $m^2 \cdot s^{-1}$ for all solutes in the backfill.

A summary of the hydraulic parameters considered in our calculations is given in Table 5-1.

The dominant mechanism for solute transport will presumably be advection, mainly driven by the high hydraulic conductivity in the fracture. Within the backfill as well as in the grout and shotcrete layers advection and diffusion may compete as dominant transport mechanisms, depending on hydraulic and/or geochemical gradients.

5.2.3 Boundary conditions

The repository depth is considered 500 m. A horizontal regional flux is assumed. Although an unsaturated transient stage will occur in the repository, while the repository is open (around 100 years), this process can not be simulated with the code we are using. Moreover, this stage represents a very small fraction of the total simulated time. The flux has been imposed by means of the boundary conditions considering a hydraulic gradient of 0.005. Upper and lower boundaries are assumed no-flow boundaries.

5.2.4 Initial conditions

Initial conditions have been only considered for the transport problem because flux is considered stationary.

The initial water compositions have been calculated by equilibrating Forsmark groundwater with the minerals of each zone (backfill, cement or granite).

The initial composition of groundwater in the fracture has been calculated by equilibrating the composition of the Forsmark reference water with calcite and pyrite, assumed to be present as fracture filling minerals in Forsmark. This pre-equilibration will avoid changes in the composition of the groundwater others than those resulting from the interaction of groundwater with the concrete and/or the backfill materials, and will simplify the interpretation of the results.

The initial concrete pore water considered in calculations has been obtained by equilibrating the Forsmark groundwater composition with the CSH Jennite ($Ca_9H_2Si_6O_{18}(OH)_8 \cdot 6H_2O$), what results in a pH value around 11.5 corresponding to a low-pH concrete /SKB 2004/. Obviously, the initial CHS phase is not well known, therefore an approximation has been made in order to meet the pH value expected by SKB for a low-pH concrete. Considering the thermodynamic data available for CSH phases, the only CSH-phase whose equilibrium lead to pH values near 11 is jennite, therefore this is the phase we consider initially present in the model. It is worth to notice that the CSH phases change with time, due to crystallisation for example, however these effects have not been considered in the model since the code PHAST do not allows it.

Table 5-1. Selected hydrodynamic parameters for the model.

Parameter	Shotcrete/grout	Backfill	Fracture
K ($m\ s^{-1}$)	$8.3 \cdot 10^{-10}$	$5.0 \cdot 10^{-11}$	$5.0 \cdot 10^{-7}$
Transmissivity ($m^2 \cdot s^{-1}$)	–	–	$2.0 \cdot 10^{-7}$
Porosity	0.3	0.363	0.2
D_e ($m^2 \cdot s^{-1}$)	10^{-10}	$1.2 \cdot 10^{-10}$	–

Al-bearing phases have not been considered in the model, the reason for that is related to the very low amount of reliable thermodynamic data for CASH phases usually present in these systems, and the need to implement kinetic dissolution rates involving Al-silicates also present in fracture-fillings and in the backfill (also including the dissolution of smectite).

In order to ensure reducing conditions the concrete water has been equilibrated with pyrite. This has caused the formation of amorphous FeS(am), calcite and torbermorite, as shown in Table 5-3.

The 30/70 mixture with MX-80 bentonite has been considered as the backfill material. The mineralogical composition of the backfill (Table 5-3) has been obtained by considering a dry density of 1.7 kg/L /SKB 2004/. Cation exchange and surface acidity reactions in the backfill, accounting for the smectite component are also considered. The exchange capacity corresponds to the bentonite fraction of the backfill (Table 5-4). The exchange coefficients (following the Gaines-Thomas convention) given in /Bradbury and Baeyens 2002/ have been used, while the acidity surface reactions constants are those reported in /Wersin 2003/ (Table 5-5). The initial bentonite pore water for the calculations has been calculated by assuming the equilibration of the Forsmark groundwater with the reactive minerals present in the backfill (Table 5-3) including cation exchange and surface acidity reactions (Table 5-4 and Table 5-5). The resulting pore water composition is listed in Table 5-2.

The calculated compositions of these groundwaters and the initial mineralogical composition in each zone of the domain are listed in Table 5-2 and Table 5-3. For any tabulated porous media in Table 5-3 there are other phases that could be considered as reactive under hyperalkaline attack, as might be feldspars, however, they are not considered in de model.

The temperature during all the calculations is fixed to 15°C, which is the actual temperature of the Forsmark groundwater.

Table 5-2. Pore water compositions considered in the model. In all cases concentration is expressed in moles/kg of water.

Element	Concrete	Backfill	Fracture
Na	90	159	89
K	$9.1\cdot10^{-1}$	1.29	$9.00\cdot10^{-1}$
Ca	28	11.9	23
Mg	$9.4\cdot10^{-1}$	4.40	9.3
C	$7.8\cdot10^{-3}$	3.09	2.15
Cl	150	153	153
S	5.3	23.4	5.20
Si	$1.6\cdot10^{-2}$	$6.63\cdot10^{-2}$	$1.85\cdot10^{-3}$
Fe	$3.1\cdot10^{-2}$	$9.46\cdot10^{-2}$	$3.30\cdot10^{-2}$
pH	11.62	7.28	7.08
Eh (mV)	–479.8	–154.9	–149.7

Table 5-3. Mineral compositions considered in the model. In all cases concentration is expressed in %wt. A value of zero means that it is not initially present but it is allowed to precipitate.

Mineral	Concrete	30/70 mixture (MX-80 bentonite)	Fracture
Amorphous FeS	0.0	0.0	0.0
Amorphous $Fe(OH)_3$	0.0	0.0	0.0
Cristobalite	0.0	0.6	0.0
Calcite	0.0021	0.0	11.5
Chalcedony	0.0	0.0	28.0
Gypsum	0.0	0.21	0.0
Portlandite	0.0	0.0	0.0
Quartz	0.0	26.1	0.0
Pyrite[1]	0.01	0.021	0.04
FeS (am)	$2.6 \cdot 10^{-6}$	0.0	0.0
Siderite	0.0	0.0	0.0
Hillebrandite	0.0	0.0	0.0
Afwillite	0.0	0.0	0.0
Jennite	10.0	0.0	0.0
Foshagite	0.0	0.0	0.0
Xonotlite	0.0	0.0	0.0
Tobermorite	0.0017	0.0	0.0
Gyrolite	0.0	0.0	0.0
Okenite	0.0	0.0	0.0
CEC (meq/100g)	0.0	22.5	0.0

[1] Pyrite is only allowed to dissolve, in case of supersaturation, amorphous FeS is allowed to precipitate instead.

Table 5-4. Exchange composition of the MX-80 bentonite /from SKB 2004/.

Components	MX-80
CEC_{bulk} (eq kg^{-1})	0.75 ± 0.02
NaX (%)	72 ± 5
KX (%)	2 ± 1
MgX_2 (%)	8 ± 5
CaX_2 (%)	18 ± 5

Table 5-5. Exchange and surface reactions considered in the model.

Exchange reactions		
Species	**Reaction (a)**	
NaX	$X^- + Na^+ = NaX$	$\log K_{eq} = 0.0$
KX	$X^- + K^+ = KX$	$\log K_{eq} = 0.60$
MgX_2	$2X^- + Mg^{2+} = MgX_2$	$\log K_{eq} = 0.34$
CaX_2	$2X^- + Ca^{2+} = CaX_2$	$\log K_{eq} = 0.41$
Surface reactions		
Species	**Reaction (b)**	
ZOH_2^+	$ZOH + H^+ = ZOH_2^+$	$\log K_{eq} = 4.5$
ZO^-	$ZOH = ZO^- + H^+$	$\log K_{eq} = -7.9$
YOH_2^+	$YOH + H^+ = YOH_2^+$	$\log K_{eq} = 6.0$
YO^-	$YOH = YO^- + H^+$	$\log K_{eq} = -10.5$

(a) Data from /Bradbury and Baeyens 2002/. (b) Data from /Wersin 2003/.

5.3 Model results

5.3.1 2D simulations considering a layer of shotcrete

The results obtained indicate that as a consequence of the concrete degradation process, pH within the shotcrete layer is maintained in the high alkaline range (pH = 11.7) and jennite, the initial CSH phase (Ca/Si = 1.5), is being replaced by tobermorite, a CSH phase with a Ca/Si ratio of 0.83 (Figure 5-3).

In the fracture, next to concrete layer, a moderate alkaline plume is developed (Figure 5-4 and Figure 5-5), with a maximum pH of 9.8 at the concrete-fracture boundary, where gyrolite, a CSH phase with a Ca/Si ratio of 0.67, precipitates (Figure 5-3).

At the same time, in the backfill, an alkaline plume is predicted to form from the tunnel walls towards the inner part of the backfill (Figure 5-4 and Figure 5-5) and gyrolite also precipitates near the contact with the concrete layer (Figure 5-3).

The predicted pH in the system, besides the concrete layer, does not reach high alkalinity values. The reason for this moderate alkalinity is that the initial state for concrete in the system was jennite and, therefore, the dissolution of alkali hydroxides [Na(OH)(s), K(OH)(s)] or portlandite prior to the dissolution of CSH has been neglected.

The predicted precipitation of gyrolite in the backfill and in the fracture is very low: less than 0.06% of the initial pore volume in both cases.

The increase in the alkalinity in the system causes precipitation of calcite (see Figure 5-6). Although calcite precipitation is not very important (less than 0.4% of the initial pore volume after 4,000 years), it is enough to cause a very important decrease in the concentration of aqueous carbonate (Figure 5-7). The maximum decrease in aqueous carbonate concentration occurs in the backfill close to the concrete layer, it concentration drops to 0.013 mmol/L from an initial value of 2.1 mmol/L.

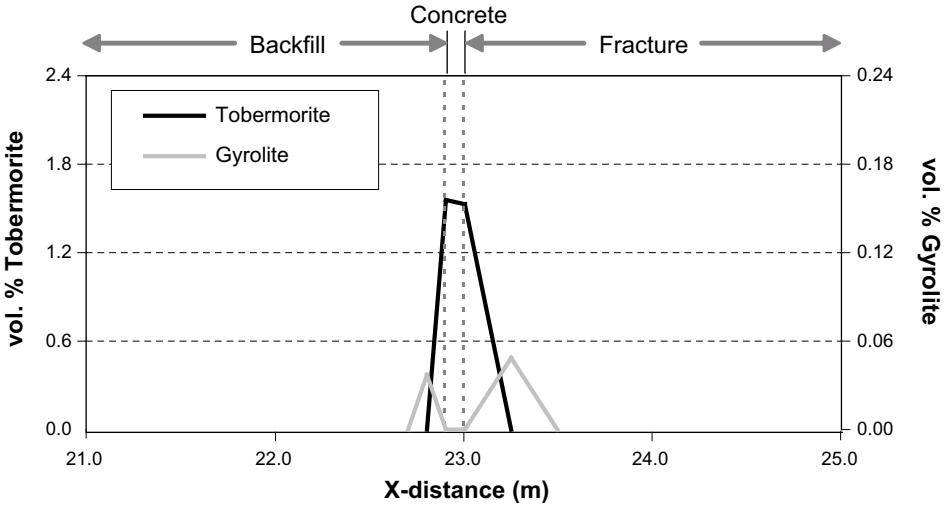

Figure 5-3. *Graphic showing the predicted amount of CSH phases after 1,000 years simulation, in volume percentage of initial pore space. Tobermorite replaces jennite in the concrete layer and gyrolite precipitates in the backfill and fracture pore space.*

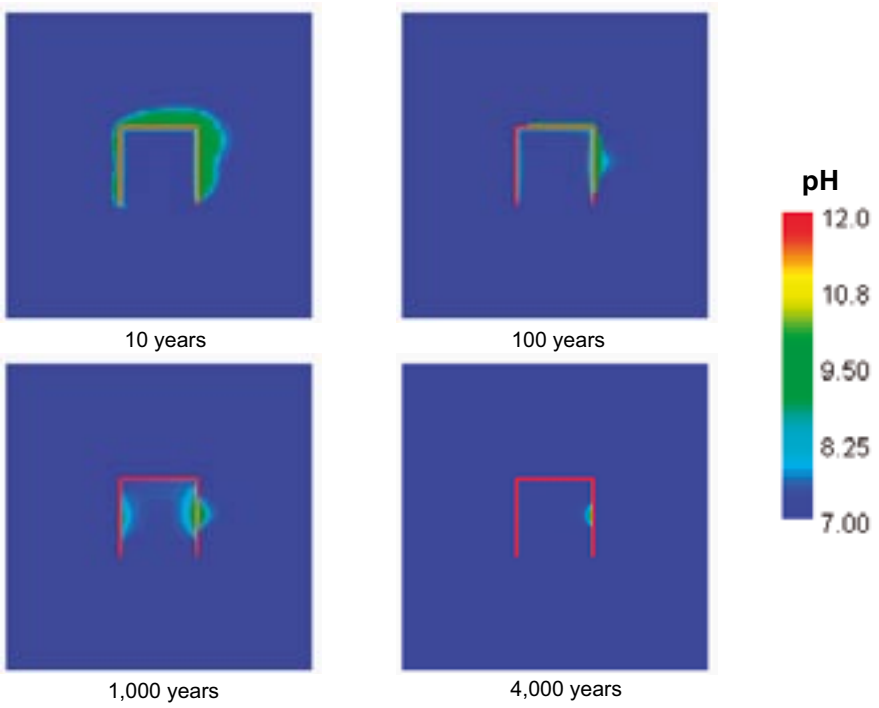

Figure 5-4. *Predicted pH evolution in the system for the shotcrete layer model.*

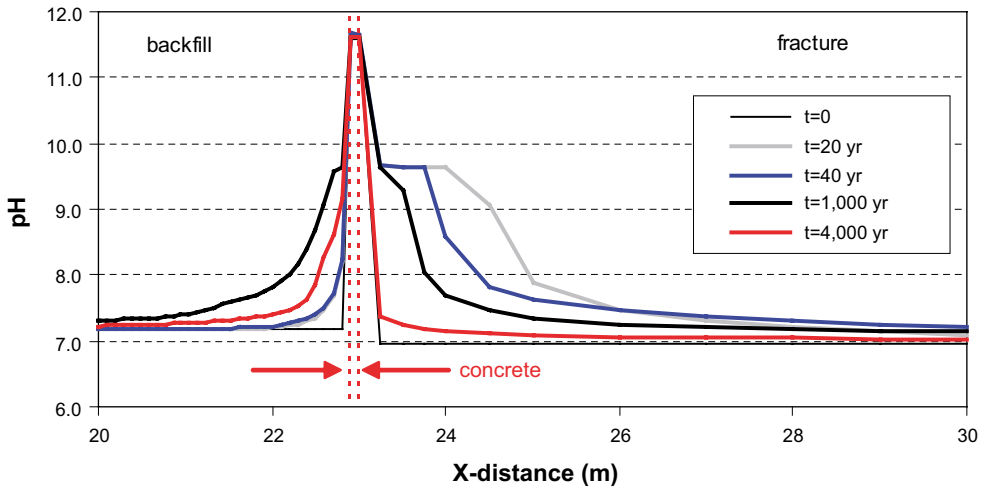

Figure 5-5. *Graphic showing the predicted pH evolution at different time intervals from the centre of the deposition tunnel, through the concrete layer and to the fracture in the flow direction.*

Another change predicted in the backfill is the complete dissolution of gypsum, as accessory mineral of the bentonite fraction. Gypsum is predicted to completely dissolve after 640 years of simulation. However, the dissolution of this mineral is also predicted in the case where no concrete is considered, and it occurs after the same simulation time. The dissolution of gypsum is linked to the need of aqueous calcium to proceed with the cation exchange reaction, where sodium is being replaced by calcium in the clay fraction of the bentonite.

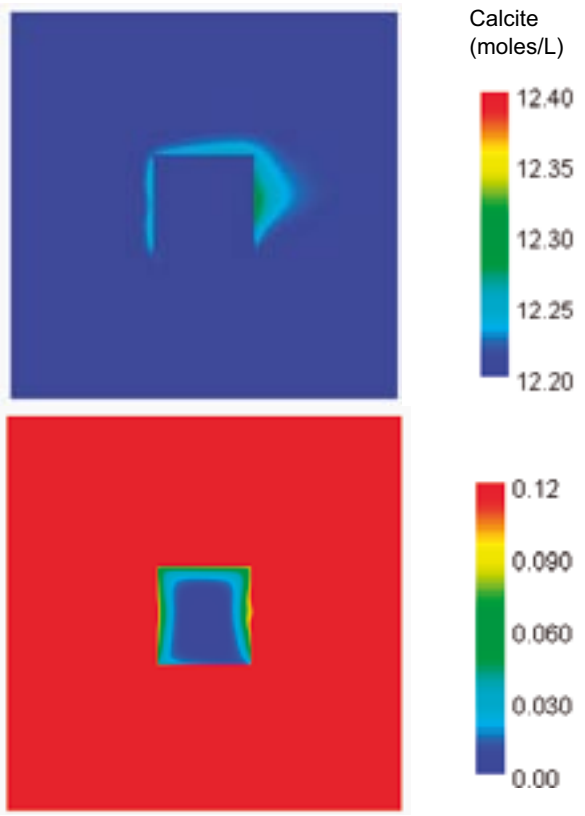

Figure 5-6. *Predicted calcite precipitation (in moles·dm^{-3} of initial porosity) after 4,000 years in the fracture zone (upper graphic) and in the backfill (lower graphic). Note the different scale for each of the graphics.*

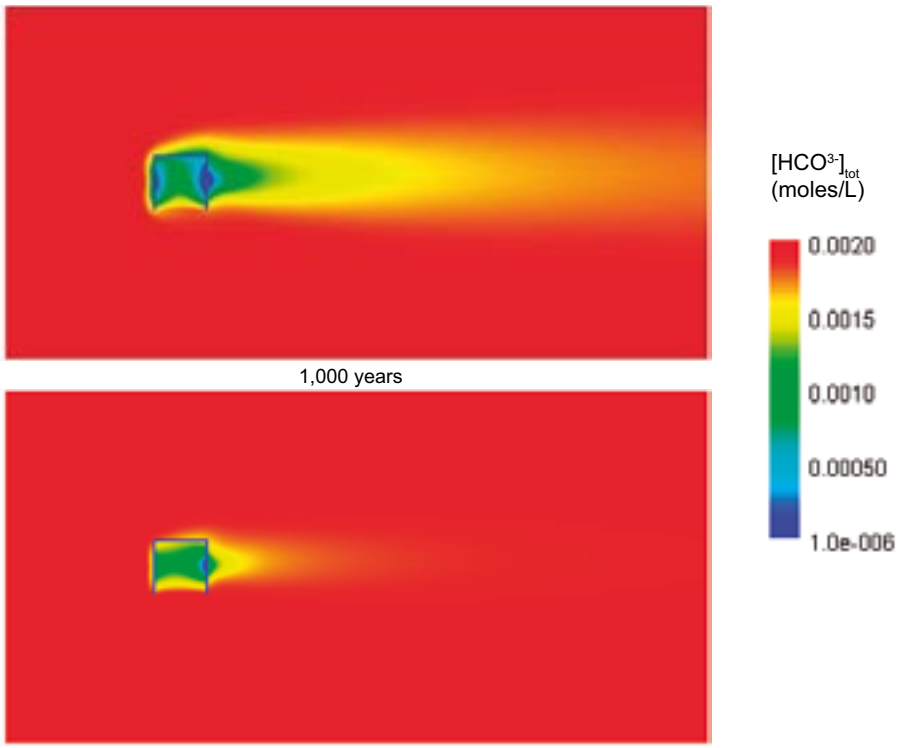

Figure 5-7. *Predicted concentration of aqueous carbonate in the system (moles/L), after 1,000 and 4,000 years of simulation.*

The higher calcium concentration in regional groundwater and concrete porewater with respect to backfill pore water represents a source of calcium, in addition to gypsum dissolution in the backfill, for the cation exchange process in the backfill. However, the evolution of the exchange process does not differ significantly when comparing the modelling results considering or not the shotcrete layer in the deposition tunnel (Figure 5-8).

According to these results, the presence of a shotcrete layer in the deposition tunnel would have no effect on the geochemical evolution of the system other than an increase in pH in the vicinity of the shotcrete. Therefore, it is not expected to alter the performance of the backfill. Nevertheless, the following uncertainties remain:

- The precipitation of CSH minerals may affect the porosity, decreasing it
- The swelling capacity may be also affected by the exchange reactions. The effects about the increase or decrease of swelling capacity are unknown.
- The initial porosity may be affected if Al-bearing phases (such as zeolites) were considered. These phases could precipitate decreasing the porosity in the fracture.

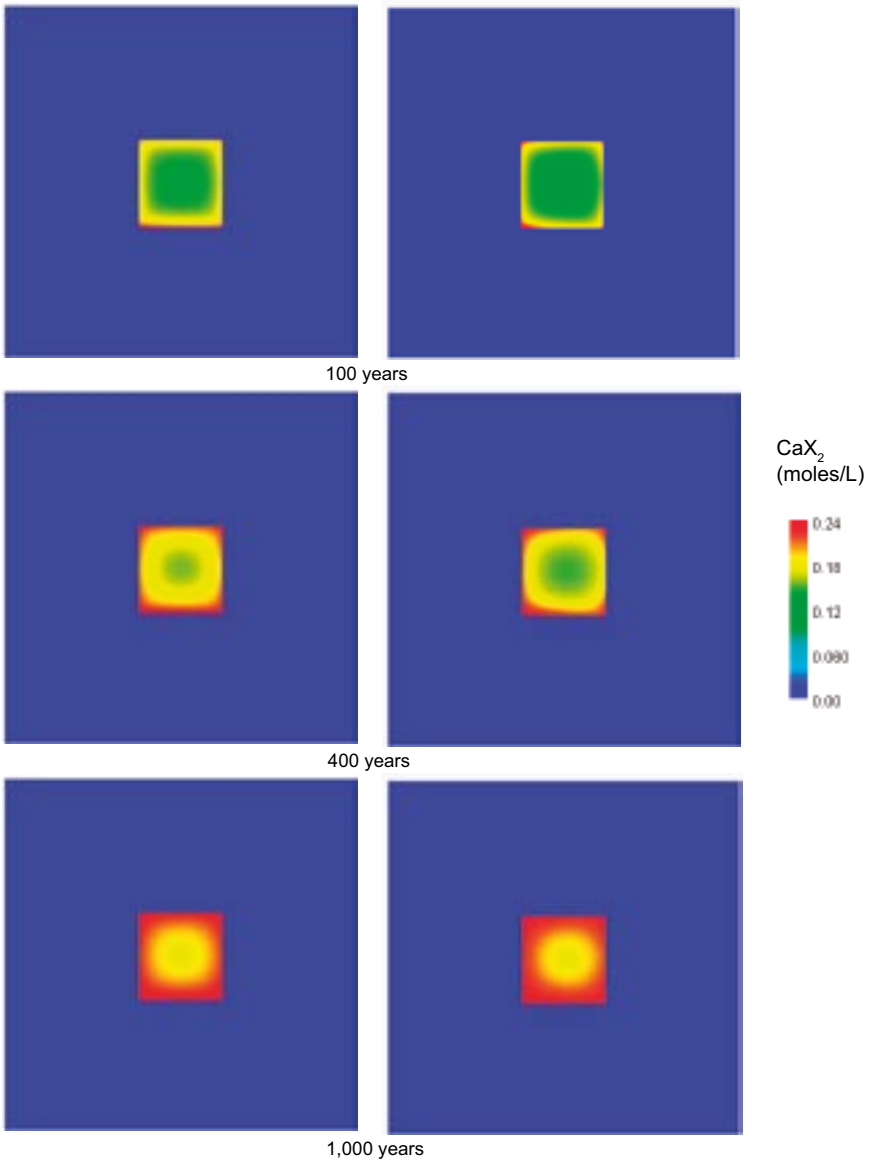

Figure 5-8. *Predicted evolution of the calcium in the exchanger of the backfill (moles/L). The graphics on the left correspond to the shotcrete layer model, whereas the graphic on the right correspond to the model without concrete.*

5.3.2 2D simulations considering a grouted fracture

The consideration of a grouted fracture around the deposition tunnel implies a large volume of concrete available for the interaction with groundwater. Thus, it is expected that the effects predicted in the previous model (shotcrete model) will be amplified. The geochemical processes driving the system are the same as in the previous model.

The main process occurring in the concrete structure is the replacement of jennite by tobermorite (Figure 5-9 and Figure 5-10), which buffers the pH to values of around 11.6 (Figure 5-11 and Figure 5-12). In the fracture, after the interaction with concrete in the flow direction, gyrolite is predicted to precipitate (Figure 5-9 and Figure 5-10). However, in this modelling case, the precipitation of gyrolite occurs in a wider area than in the previous shotcrete model (Figure 5-3).

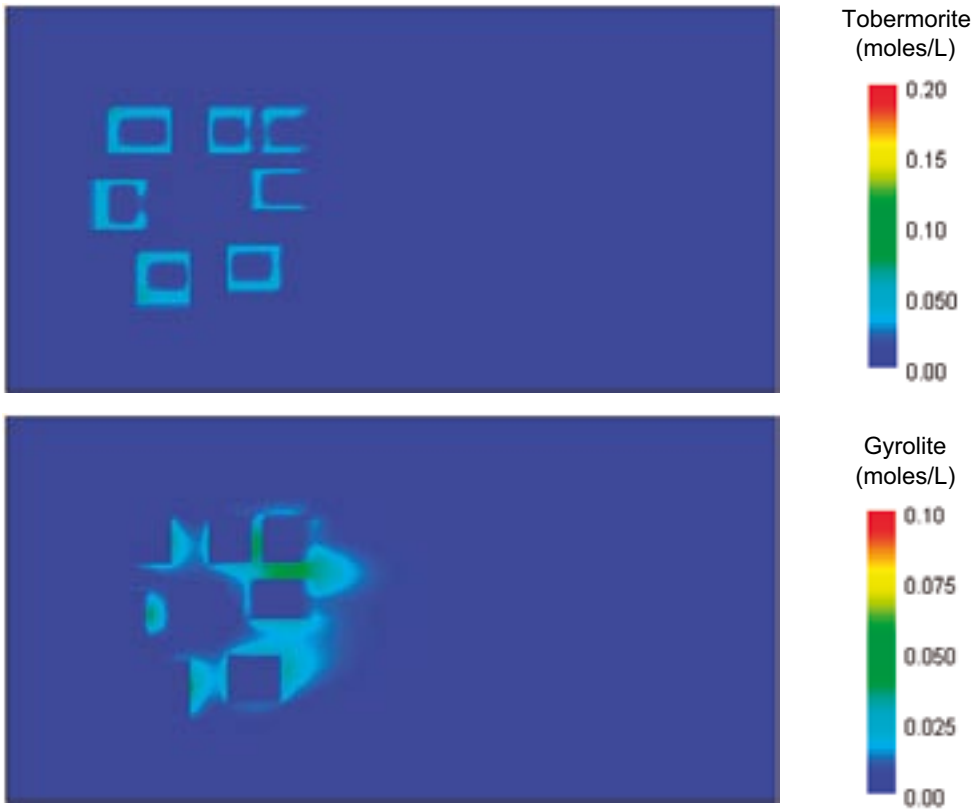

Figure 5-9. *Graphics showing the predicted distribution of newly formed CSH phases after 1,000 years. Tobermorite is replacing jennite within the concrete (upper graphic) and gyrolite precipitates in the fracture pore space around the concrete (lower graphic). Units are moles·dm^{-3} of initial porosity.*

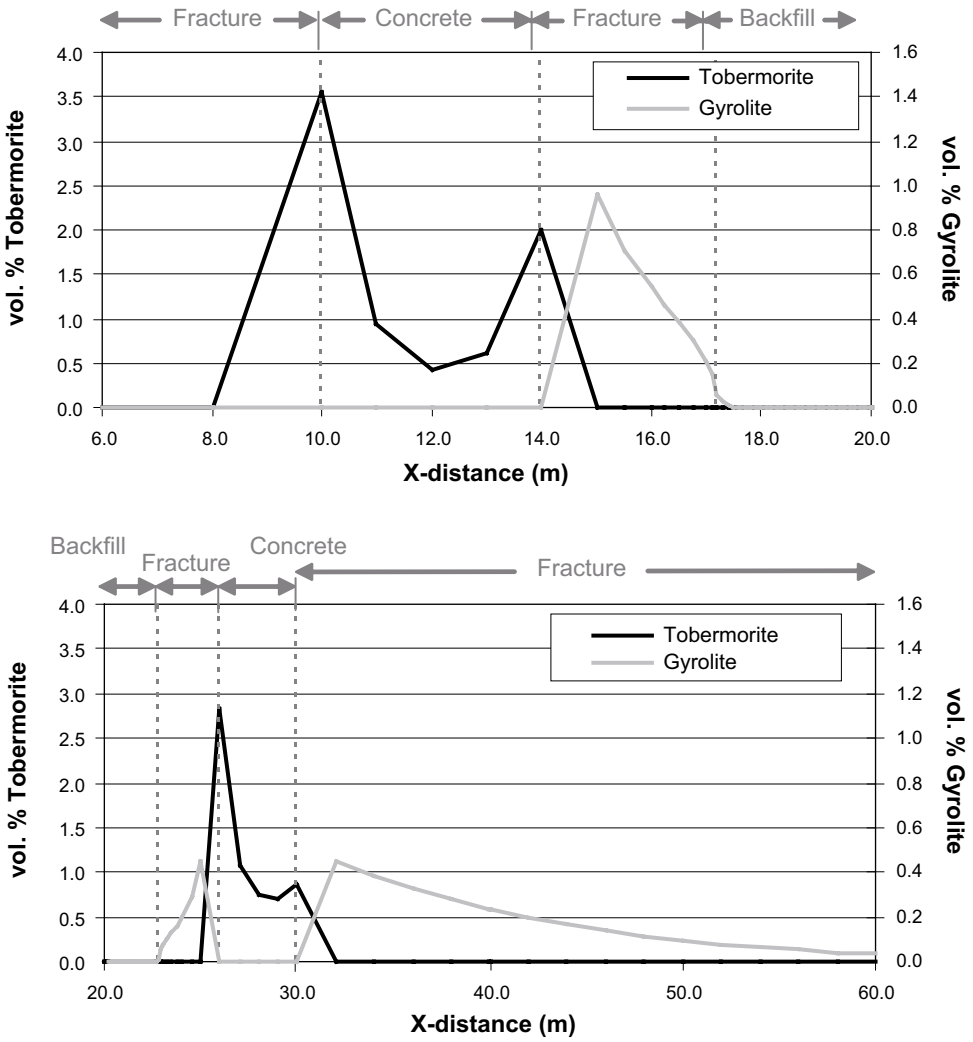

Figure 5-10. *Graphics showing the predicted precipitation of tobermorite and gyrolite in volume percentage of initial porosity after 4,000 years simulation. The upper graphic shows the first concrete structure found by groundwater in the flow direction, where tobermorite is replacing jennite and gyrolite is predicted to precipitate in the fracture and minor amounts in the backfill after the interaction with concrete. In the lower graphic gyrolite also precipitates in the fracture, but a larger precipitation plume is predicted.*

The development of an alkaline plume in this modelling case is also larger than in the previous case (Figure 5-11), although the maximum pH value in the fracture zone is the same as in the shotcrete model (pH = 9.8). In the backfill, however, CSH phases only precipitate after very long simulation times and in very low amounts ($< 4 \cdot 10^{-3}$ moles/L) close to the fracture-backfill boundary. This is because these phases are mainly formed inside the concrete structure and their precipitation slowly propagates with time away from these structures.

Therefore, precipitation of gyrolite starts in the backfill after 1,500 years of simulation time, at the fracture-backfill boundary and reaches a maximum penetration depth of 0.3 m into the backfill (Figure 5-13).

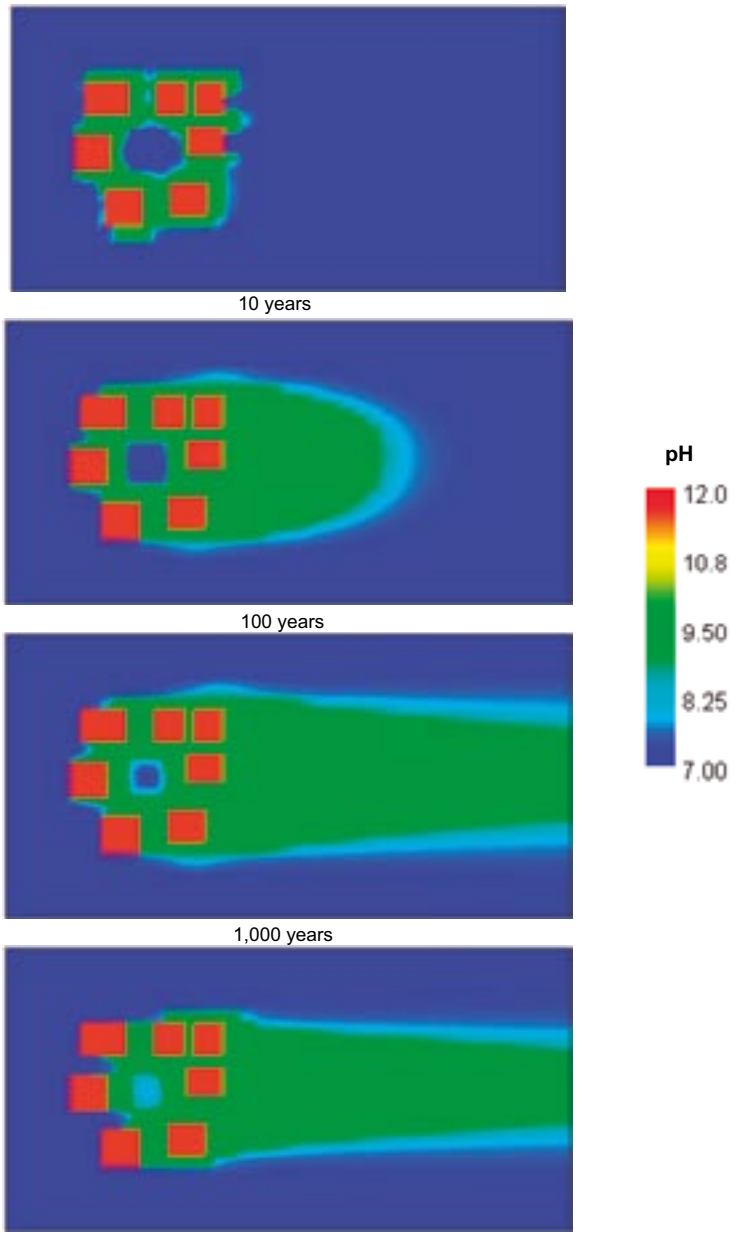

Figure 5-11. *Predicted pH evolution in the system considering a fracture partially grouted.*

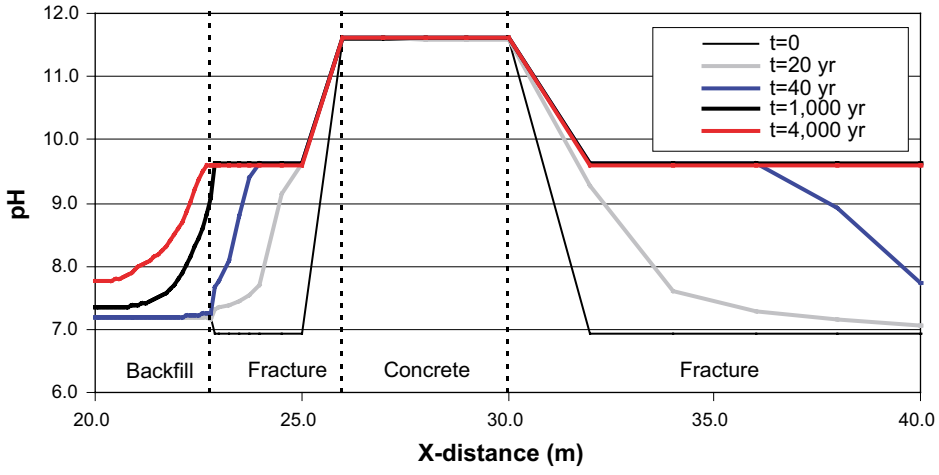

Figure 5-12. *Predicted pH evolution in the backfill and around a concrete structure.*

Another difference with respect to the previous modelling case is the pH evolution in the backfill. In the present case, higher pH values are reached, although they are never higher than 10 (see Figure 5-12).

As in the shotcrete modelling case, the aqueous carbonate concentration is much depleted in the area of influence of the high alkalinity plume (Figure 5-14). Again, in the present case this decrease in the carbonate concentration is related to the precipitation of calcite caused by the pH increase (Figure 5-15).

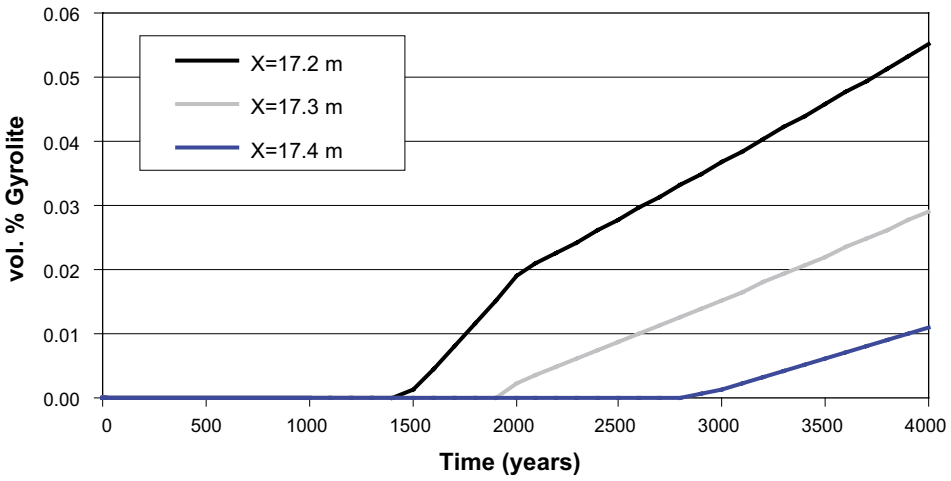

Figure 5-13. *Graphic showing the predicted precipitation of gyrolite as a function of time (volume percentage of the initial pore space) at different locations in the backfill: At the fracture-bentonite boundary (X = 17.2 m), and at 0.1 and 0.2 m from this boundary inside the backfill (X = 17.3 m and X = 17.4 m, respectively).*

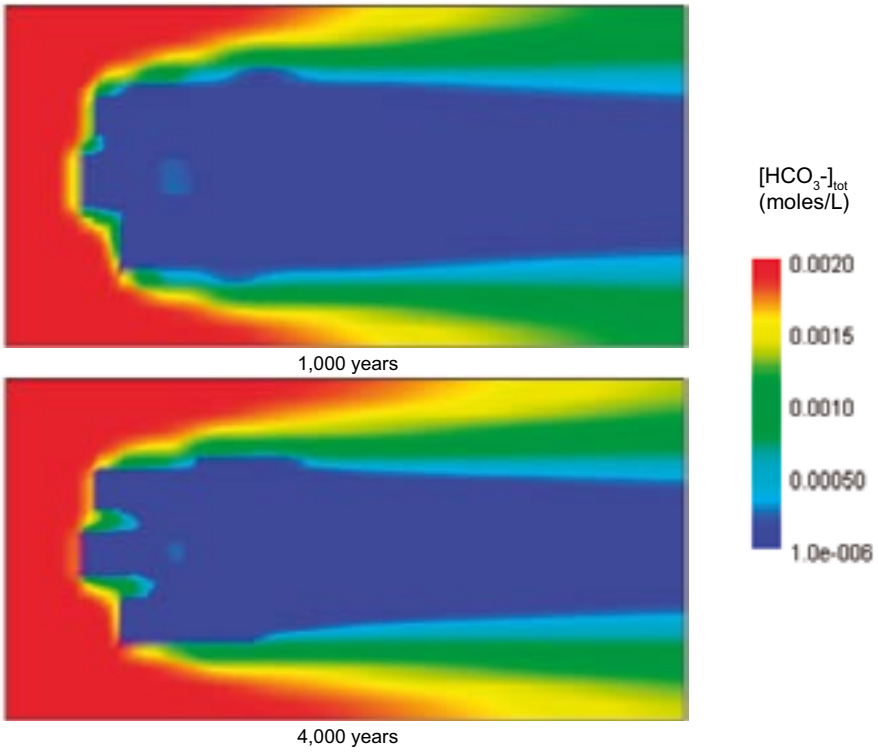

Figure 5-14. *Predicted aqueous carbonate concentration after 1,000 and 4,000 years of simulation respectively (moles/L). Note the larger plume of depleted carbonate in comparison with that in Figure 5-7.*

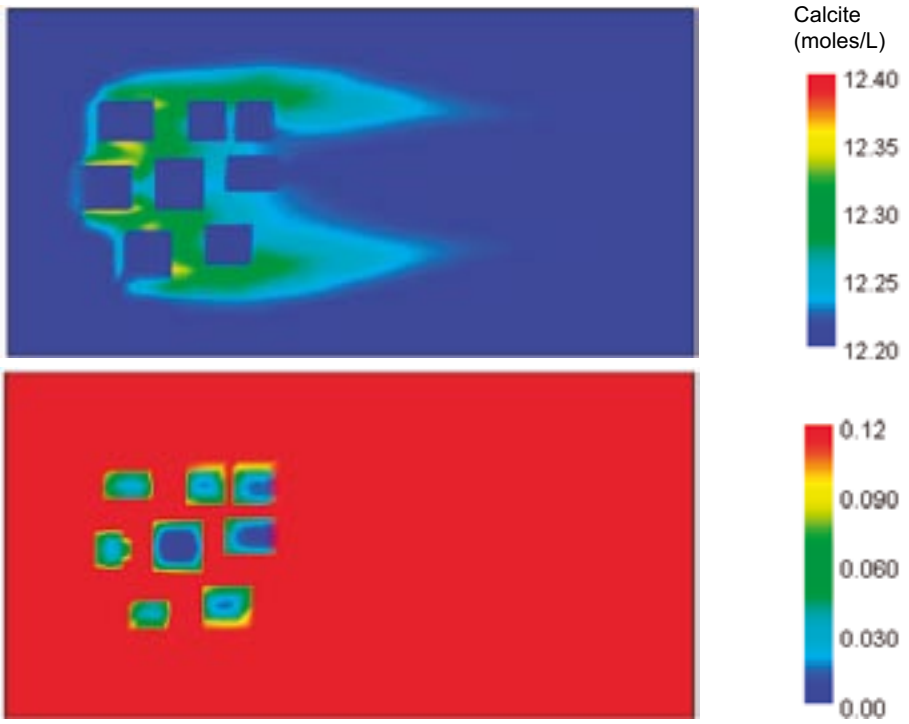

Figure 5-15. *Predicted calcite precipitation (in moles·dm^{-3} of initial porosity) after 4,000 years in the fracture zone (upper graphic) and in the backfill (lower graphic). Note the different scale for each of the graphics.*

In the present modelling case, the change in the composition of the exchanger in the clay fraction of the backfill follows the same evolution predicted in both the shotcrete modelling case and the model without concrete. The model predicts that sodium is being replaced mainly by calcium (Figure 5-16), but in the present case it seems that this replacement is slightly faster than in the shotcrete model. The replacement reaches a maximum after 700 years. This affects the dissolution of gypsum, as a source of calcium for the exchange process. In the present case, the total dissolution of gypsum is achieved after 600 years, slightly earlier than in the shotcrete case.

The geochemical evolution of the backfill indicates that the most important process is the cation exchange, whereas the pH is buffered by the equilibrium with calcite. As the high alkalinity plume also affects the backfill pore water, it is possible that larger amounts of calcite and other minerals (i.e. CSH phases) can modify the porosity of the backfill, decreasing it and leading to changes in the transport parameters. However, the replacement in the exchanger can also modify the swelling capacity of the bentonite fraction of the backfill, which can result in additional modifications of the initial porosity. Unfortunately, we are not able to evaluate the porosity changes due to variations on the swelling capacity of the bentonite, although we can assume that at the final dry densities expected for bentonite under repository conditions, the variations on the swelling capacity of bentonite will be not very different.

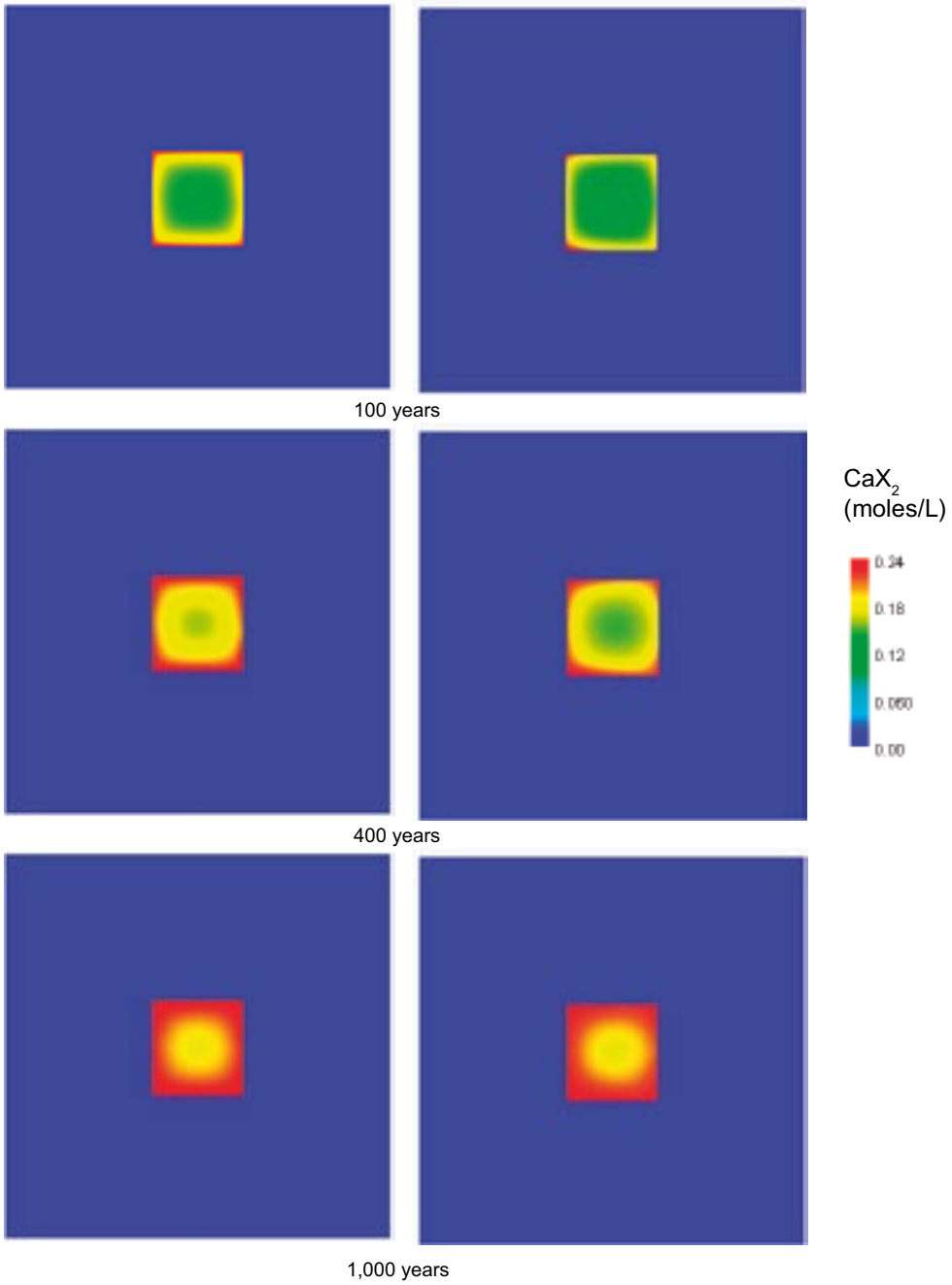

Figure 5-16. *Predicted evolution of the calcium in the exchanger of the backfill. The graphics on the left correspond to the grouted fracture model, whereas the graphic on the right correspond to the model without concrete.*

6 Conclusions

The modelling results show that the presence of low-pH shotcrete and grout has no major effects on the backfill performance. A high pH plume can be developed on the conductive fractures intersected by the deposition tunnel and to a minor extent also in the backfill material. The development of these alkalinity plumes leads to the precipitation of CSH phases and calcite in both the fracture and the backfill. The precipitation of these minerals can reduce the initial porosity by less than 1%.

In the backfill there is a replacement of Na by Ca in the cation exchange sites of smectite, which can potentially affect its swelling capacity. However, this exchange process is not related to the presence of concrete, as it also occurs when no concrete is considered. In any case, it is difficult to evaluate the variation of the swelling capacity due to the exchange process, as under the expected dry densities in repository conditions is likely that these changes will be of minor importance.

In addition, a series of other phases not considered in the modelling cases, as feldspars, should be taken into account. Among these phases are CSH gels and other aluminium bearing phases normally present in the concrete and which can also precipitate in the fracture and in the backfill. Also the inclusion of iron in the system and the potential precipitation of iron oxyhydroxides and sulphides could result in a substantial improvement of the model, which in turn can control the redox evolution of the system.

Finally, the consideration of a 3D model, where the deposition tunnel can be extended, would be advisable. It can result in changes in the minerals precipitated related to the transport of solutes in a third dimension, away from the fracture zone, modifying the concentration gradients that control diffusive transport.

Although the high temperature in the system will probably not have any major geochemical effects it is advisable to take it into account forward in new modelling exercises.

7 References

Atkins M, Glasser F P, 1992. Application of Portland cement-based materials to radioactive waste immobilisation. Waste Management 12: 105–135.

Atkinson A, 1985. The time dependence of pH within a repository for radioactive waste disposal. AERE Report R-11777, Harwell, UK.

Bensted J, 1999. Thaumasite: background and nature in deterioration of cements, mortars and concretes. Cement and Concrete Composites 21:117–121.

Bradbury M H, Baeyens B, 2002. Pore water chemistry in compacted re-saturated MX-Bentonite. Physico-chemical characterisation and geochemical modelling. Paul Scherrer Institut publications, PSI Bericht, Nr 2002-10.

Brown P W, Bothe Jr J V, 1993. The stability of ettringite. Advances in Cement Research, 5 No. 18: 47–63.

Clodic L, Meike A, 1997. Thermodynamics of calcium silicate hydrates. Development of a database to model concrete dissolution at 25°C using the EQ3/6 geochemical modeling code. LLNL Report UCRL-ID-132088.

Czernin W, 1969. Zementchemie für Bauingenieure. Bauverlag GMbH, Weisbaden-Berlin.

Damidot D, Atkins M, Kindness A, Glasser F P, 1992. Sulphate attack on concrete: limits of the Aft stability domain. Cement and concrete research, 22:229–234.

Delagrave A, Pigeon M, Revertégat E, 1994. Influence of chloride ions and pH level on the durability of high performance cement pastes. Cement and Concrete Research 24:1433–1443.

Dershowitz W, Winberg A, Hermansson J, Byegard J, Tullborg E-L, Andersson P, Mazurek M, 2003. Äspö Hard Rock Laboratory. Äspö Task Force on modelling of groundwater flow and transport of solutes. Task 6C. A semi-synthetic model of block scale conductive structures at the Äspö HRL. SKB International progress report IPR-03-13.

Engkvist I, Albinsson Y, Johansson W, 1996. The long-term stability of cement-leaching tests. SKB TR 96-09, Svensk Kärnbränslehantering AB.

Font O, Querol X, Plana F, Lopez-Soler A, Chimenos J M, March M J, Espiell F, Burgos S, Garcia F, Alliman C, 2001. Occurrence and distribution of valuable metals in fly ash from Puertollano IGCC power plant, Spain. 2001 International Ash Utilization Symposium, paper number 38, Center for Applied Energy Research, University of Kentucky.

Hartley L, Cox I, Holton D, Hunter F, Joyce S, Gylling B, Lindgren M, 2004. Groundwater flow and radionuclide transport modelling using CONNECTFLOW in support of the SR Can assessment. SKB R-04-61, Svensk Kärnbränslehantering AB.

Hoek E, Brown E T, 1995. Practical estimates of rock mass strength. Int. Journal of Rock Mechanics and Mining Sciences, 34:1165–1186.

Hoek E, 2000. Practical Rock Engineering, chapter 15, p.276–288, not published (www.rocscience.com/hoek/PracticalRockEngineering.asp).

Höglund L O, 2001. Project SAFE. Modelling of the long-term concrete degradation processes in the Swedish SFR repository. SKB R-01-08, Svensk Kärnbränslehantering AB.

Holmén J G, Stigsson M, 2001. Modelling of future hydrogeological conditions at SFR. SKB R-01-02, Svensk Kärnbränslehantering AB.

Huang W, 2001. Improving the properties of cement fly ash grout using fiber and superplasticizer. Cement and Concrete Research, 31:1033–1041.

Idorn G M, Henriksen K R, 1984. State of the art for fly ash uses in concrete. Cement and Concrete Research. 14:463–470.

Jolicoeur C, Simard M, 1998. Chemical Admixture-Cement Interactions: Phenomenology and Physico-chemical concepts. Cement and Concrete Composites 20:87–101.

Kipp K L, 1997. Guide to the revised heat and solute transport simulator, HST3D-version 2. U.S. Geological Survey Water Resources Investigations report 97-4157, 149 pp.

Lagerblad B, Trägardh J, 1994. Conceptual model for concrete long time degradation in a deep nuclear waste repository, Swedish Cement and Concrete Research Institute. SKB TR 95-21, Svensk Kärnbränslehantering AB.

Lagerblad B, 1999. Long term test of concrete resistance against sulphate attack. In: "Sulphate Attach Mechanisms", Marchand, J. and Skalny, J.P., (Eds.), Materials Science of concrete (special volume), The American Ceramic Society, Westerville OH, USA.

Lagerblad B, 2001. Leaching performance of concrete based on samples from old concrete constructions. SKB TR-01-27, Svensk Kärnbränslehantering AB.

Lagerblad B, Jennings H M, Chen J J, 2003. Modification of cement paste with silica fume – A NMR Study, 1st International Symposium on Nanotechnology in Construction, Paisly. June 2003, In press conference volume, Royal Society of Chemistry.

Lagerblad B, 2005. Carbon dioxide uptake during concrete life cycle-state of the art. CBI report 2:2005.

Midness S, Young J F, 1981. Concrete. Englewood Cliffs, N.J.: Prentice-Hall, Inc.

Mor A, Mehta P K, 1984. Effect of superplasticizing admixtures on cement hydration. Cement and Concrete Research, 14:754–756.

Neville A M, 1981. Properties of concrete. Pitman publ. LTD, pp 1–779.

Oliver J P, Massat M, 1992. Permeability and microstructure of concrete: a review of modelling. Cement and Concrete Research 22: 503–514.

Page C L, Short N R, Tarras A, 1981. Diffusion of chloride ions in hardened pastes. ement and Concrete Research, 11:395–406.

Parkhurst D L, Appelo C A J, 1999. User's guide to PHREEQC (version 2) – A computer program for speciation, batch-reaction, one-dimensional transport and inverse geochemical calculations. U.S. Geological Survey Water Resources investigations report 99-4259.

Parkhurst D L, Kipp K L, Engesgaard P, 2000. PHAST. A program for simulating groundwater flow and multicomponent geochemical reactions. User's guide, USGS, 154 pp.

Pereira A, Sundström B, 2004. Two dimensional near-field calculations of radionuclide releases from the SFL 3 and SFL 5 repository. SKI report 2004:36.

Pointeau I, 2001. Etude mécanistique et modelisation de la retention de radionucléides par les silicates de calcium hydratés (CSH) des ciments. Thèse Doctorale Université Reims Champange-Ardenne, Collection Les Rapports, ANDRA.

Prudêncio L R, 1998. Accelerating Admixtures for Shotcrete. Cement and Concrete Composites 20:213–219.

Revertegat E, Adenot F, Richet C, Wu L, Glasser F P, Damidot D, Stronach S A, 1997. Theorical and experimental study of degradation mechanisms of cement in the repository environment. Report EUR 17642 EN. Official Publications of the European Communities, Luxemburg.

Shehata M H, Thomas M D A, 2000. The effect of fly ash composition on the expansion of concrete due to alkali-silica reaction, Cement and Concrete Research 30 (7): 1063–1072.

Sievänen U, Syrjänen P, Ranta-aho S, 2005. Injection grout for deep repositories-Low-pH cementitious grout for larger fractures. Posiva Oy, Olkiluoto, Finland. Posiva Working-Report 2004-47.

SKB, 2004. Interim initial state report for the safety assessment SR-Can. SKB R-04-35, Svensk Kärnbränslehanteirng AB.

SKB, 2006. Long-term safety for KBS-3 repositories at Forsmark and Laxemar – a first evaluation. Main Report of the SR-Can project. SKB TR-06-09. Svensk Kärnbränslehantering AB.

Tang, Nilsson, 1993. A study of the quantitative relationship between permeability and pore size distribution of hardened cement pastes. Cement and Concrete Research, vol. 22, pp 541–550, 1992.

Taylor H F W, 1990. Cement chemistry. Academic Press. Thomas Telford Publishing, London.

Wersin P, 2003. Geochemical modelling of bentonite pore water in high-level waster repository. Journal of Contaminant Hydrology, 61, 405–422.

Young J F, 1972. A review of the mechanisms of set-retardation in Portland cement pastes containing organic admixtures. Cement and Concrete Research 2:415–433.

Zhang M H, 1995. Microstructure, crack propagation, and mechanical properties of cement pastes containing high volumes of fly ashes. Cement and Concrete Research, 25 (6): 1165–1178.

Zhou F P, Barr B I G, Lydon F D, 1995. Cement and Concrete Research, 25 (3): 543–552.

Appendix A

Concrete structure, additives and shotcrete components

Structure of concrete

The structure of concrete is formed by three phases: aggregates cement-hydrated paste and the transition zone. The last one is defined as a thin layer (micrometric order) formed around the grains that separates aggregate and cement paste (Figure 1). The transition zone is the weakest phase in the cement structure and it becomes unstable with time /Taylor 1990/. The transition zone controls the elasticity and strength of concrete, its power of retraction and its fluency.

The structure of concrete is developed in short time and it will evolve slowly along its life-time /Taylor 1990/. Initially, the dissolution of gypsum and aluminates release Ca^{2+}, SO_4^{2-}, $Al_2O_y^-$ and OH^- whose combination produce primary ettringite ($C_6A\underline{S}H_{32}$). Later, hexagonal crystals of $Ca(OH)_2$ (portlandite) will grow rapidly and, in short time, a structure of amorphous CSH begins to form. Depending on the spatial availability, two types of texture will develop (hive or fibrous) and this structure evolves to a denser one due to a heavy crystallization of new internal CSH crystals. Finally, ettringite will evolve to monosulfoaluminate.

Three stages, defined during concrete hydration, determine the concrete structure: dormant period, setting and hardening /Pointeau 2001/.

The dormant period is defined during the first minutes of hydration (half an hour as maximum) and it is characterized by the start of the formation of the transition zone through growing of ettringite and portlandite. Later, during the setting period, the CSH phases develop and concrete begins to define its mechanical properties, completely established during the last phase of hydration, named hardening. The setting period lasts some days while hardening takes several weeks (Figure 2).

The structure of concrete will control its mechanical strength and a good development of the transition zone is a key factor in obtaining better structural features. Before fracturing, the components of concrete behave elastically, although concrete is inelastic. That means that concrete is highly resistant under compression although under tensile stresses it behaves weakly /Hoek and Brown 1995/. Shotcrete behaves similarly; its mechanical resistance is not as high as for conventional concrete, though.

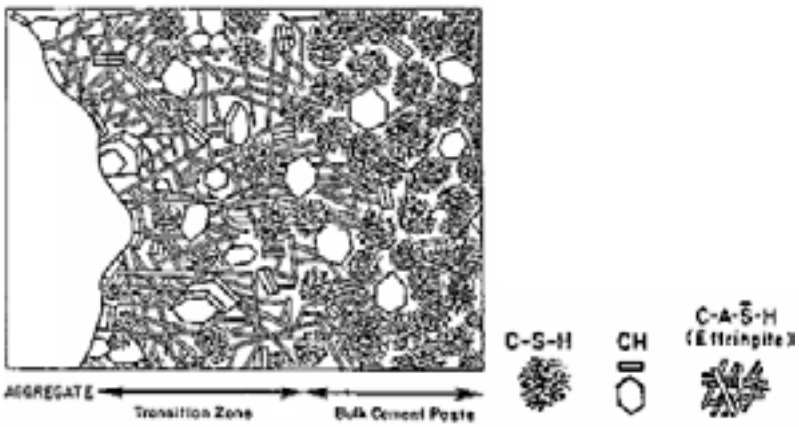

Figure 1. *Diagrammatic representation of the transition zone and bulk cement paste in concrete /Pointeau 2001/.*

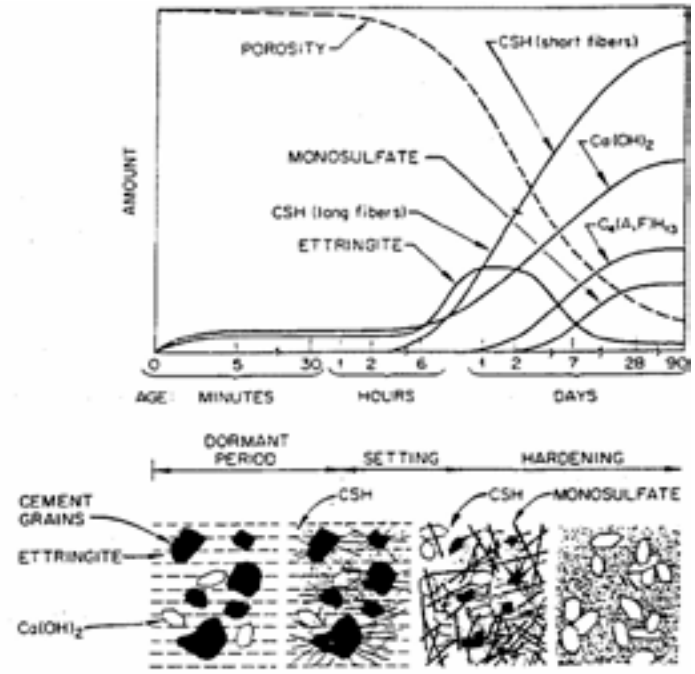

Figure 2. *Phases controlling the concrete structure development during the hydration process /Pointeau 2001/.*

Cement admixtures

Cement admixtures are substances added to the cement paste during concrete preparation that can alter the original properties of concrete. Concrete still presents several drawbacks in its behaviour like poor workability, high shrinkage cracks, poor performance against chemicals, high permeability and inadequate protection of steel reinforcement from corrosion, low tensile strength and low fracture toughness. The cement admixtures are expected to overcome these deficiencies.

For special grouts like shotcrete or injected grouts most of the admixtures used are superplasticizers as additive and silica fume as addition. In shotcrete however, the use of steel fibres is also considered (see next section).

A summary of cement admixtures for concrete, composition and the effects over the concrete functionality is presented in Table 1.

Shotcrete components

Cement

Cement is required in doses of 400 and 450 kg of cement by m^3 of concrete (UNE-80607). Cement content can be modified by using other fine materials such as silica fume (pozzolans). Requirements about cement admixtures and proportions change as a function of shotcrete application.

Pozzolanic admixtures

A pozzolan is a siliceous or siliceous-aluminous material that becomes cementitious when combined with an activator, like OPC, in presence of water. The pozzolan substitutes the OPC and it is added in high proportion to the cement paste (as high as 20% in weight). The most habitual pozzolan materials used in shotcrete and concrete in general are silica fume and fly ash.

Table 1. Type of admixture used in cement pastes and effects over concrete performance (www.admixtures.org.uk).

Type of admixture	Effects	Material
Accelerators	Accelerate setting and early strength development	Calcium chloride, triethanolamine, sodium thiocyanate, calcium formate, calcium nitrite, calcium nitrate
Air detrainers	Decrease air content	Tributyl phosphate, dibutyl phthalate, octyl alcohol, water-insoluble esters of carbonic and boic acid, silicones
Air-entraining	Improve durability in environments of freeze-thaw, deicers, sulphate and alkali reactivity. Improve workability	Salts of wood resins, lignin, petroleum acids, proteinaceous material or sulphonated hydrocarbons. Some synthetic detergents. Fatty and resinous acids and their salts. Alyklbenzene sulphonates
Alkali-reactivity reducers	Reduce alkali-reactivity expansion	Pozzolans, blast-furnace slag, salts of lithium and barium, air-entraining agents
Bonding	Increase bond strength	Rubber, polyvinyl chloride, polyvinyl acetate, acrylics, butadienestyrene copolymers
Corrosion inhibitors	Reduce steel corrosion activity in a chloride environment	Calcium nitrite, sodium nitrite, sodium benzoate, certain phosphates or flurosilicates, fluroaluminates
Damp proofing	Retard moisture penetration into dry PCC	Soaps of calcium or ammonium stearate or oleate. Butyl stearate. Petroleum products
Natural pozzolans	Pozzolonic activity	Diatomaceous earth, opaline cherts, clays, shales, volcanic tuffs, pumicites
	Improve workability, plasticity, sulphate resistance	Fly ash (classes C and F)
	Reduce alkali reactivity, permeability, heat of hydration	Silica fume
	Partial cement replacement	
	Filler	
Cementitious minerals	Hydraulic properties	Ground granulated blast-furnace slag. Natural cement. Hydraulic hydrated lime
	Partial cement replacement	
Inert minerals	Improve workability. Filler	Marble, dolomite, quartz, granite
Permeability reducers	Reduce permeability	Silica fume, fly ash, ground slag, natural pozzolans, water reducers, latex
Pumping aids	Improve pumpability	Organic and synthetic polymers. Organic flocculents. Organic emulsions of paraffin, coal tar, asphalt, acrylics. Bentonite and pyrogenic silicas. Natural pozzolans. Fly ash. Hydrated lime
Set-retarders	Retard setting time during hydration	Lignin, borax, sugars, tartaric acid and salts
Superplasticizers (high-range water reducers)	Reduce water-cement ratio by a minimum of 12%. Increase workability at low water-cement ratios	Sulphonated melamine formaldehyde condensates. Sulphonated naphthalene formaldehyde condensates. Lignosulphonates
Water reducer	Reduce water demand by a minimum of 5%	Lignosulphonates. Hydroxylated carboxylic acids. Carbohydrates
Workability agents	Improve workability	Air-entraining admixtures. Cementitious materials, natural pozzolans and inert minerals (except silica fume)

a) Silica Fume

Silica fume is a very fine non-crystalline pozzolanic material composed mostly of silica. Addition of silica fume to cement varies between 5 and 10% of cement weight, however, in some cases additions as high as 20% are allowed /Zhou et al. 1995/. Silica fume is a byproduct of producing silicon metal or ferrosilicon alloys in electric furnaces. The raw materials are

quartz and coal. The smoke that results from furnace operation is collected and sold as silica fume, rather than being landfilled. Silica fume consists primarily of amorphous (non-crystalline) silicon dioxide (SiO_2). The individual particles are extremely small, approximately $1/100^{th}$ the size of an average cement particle.

Silica fume is added to increase the mechanical strength of shotcrete, reducing its permeability and increasing its resistance to sulphate attack. The use of silica fume improves the bond strength of shotcrete to the substrate and between the different layers obtaining a more cohesive material.

The material is more resistant to washout, where fresh shotcrete is subjected to the action of flowing water, and rebound is significantly reduced. In general, silica-fume shotcrete produces unhardened and hardened material properties which, among other uses, make it suitable as a substitute for polymer-modified shotcrete and accelerated shotcrete applications. Silica-fume shotcrete is widely used often combined with fibres to control the shrinkage cracking.

b) Fly ash

Fly ash is a fine grained material residue resulting from combustion of ground and powdered coal at the electric generating plants. It consists of organic and inorganic matter present in coal that has been fused during coal combustion. This material solidifies while suspended in the exhaustion gases, and is collected by electrostatic precipitators. Since the particles solidify while suspended in the gases, fly ashes are generally very fine (silt size 0.074–0.005 mm) and spherical in shape. These small particles are highly inert, and when they are used as an addition, the concrete gains compaction and impermeability. The Substitution of OPC by fly ash in shotcrete is similar to silica fume; however, in normal concrete this substitution may be as high as 60% in cement weight /Zhang 1995/.

Based on the chemical composition of fly ashes they can be classified into two Groups: C and F (Tables 2 and 3). Fly ashes of class C comes from lignite and sub-bituminous burned coals, whereas fly ashes of class F are products of anthracite and bituminous burned coals /Idorn and Henriksen 1984/. Class C, or lime-rich fly ash, is readily activated by its own lime-content and by the $Ca(OH)_2$ released during the Portland cement hydration. Class F, or lime-poor fly ash, is readily activated at first by the alkalis released by the Portland cement after mixing and during the early hydration. This classification will control its chemical composition that varies only slightly from one to other fly ash type.

Combustion of coals could imply the presence of elements such as Pb, V, Zn, Ni, As, Ge, and Ga among others. Thus, heavy metals are not rejected in some fly ashes compositions. Analysis of fly ashes providing from the Puertollano IGCC power plant in Spain show that the major crystalline phases are Pb, Zn and Fe sulfides (galena, sphalerite and würtzite, and pyrrhotine, respectively) /Font et al. 2001/. This fact could imply a potential contaminant factor if ground-water interacts with the concrete used in the repository. Thus, this possibility must be considered in the repository assessment. A good choice of coal to be burned in the electric-generating plants is crucial to obtain fly ashes of optimal chemical composition.

Table 2. Typical fly ashes classification /Shehata and Thomas 2000/.

Fly ash class CLASS F	CLASS C	Properties
70%	50%	SiO_2; Al_2O_3; Fe_2O_3 minimum values in %
5%	5%	Sulphur trioxide (SO_3) maximum values in %
3%	3%	Moisture content maximum values in %
6%	6%	Loss on ignition maximum values in %

Table 3. Chemical composition of some American fly ashes /Zhang 1995/.

	Class F ash Georgia % (in weight)	Class C ash North Dakota % (in weight)
Silicon dioxide (SiO_2)	53.64	46.20
Aluminium oxide (Al_2O_3)	27.42	15.60
Ferric oxide (Fe_2O_3)	7.74	7.70
Calcium oxide (CaO)	2.88	14.93
Magnesium oxide (MgO)	0.99	4.34
Sodium oxide (Na_2O)	0.38	5.52
Potassium oxide (K_2O)	2.42	1.86
Phosphorous oxide (P_2O_3)	0.34	0.18
Titatium oxide (TiO_2)	1.66	0.74
Manganes oxide (MnO)	0.02	0.03
Sulphur trioxide (SO_3)	0.37	1.72
Loss on ignition	1.49	0.45
Total	**99.35**	**99.27**

Aggregates

The granulometric classification used for shotcrete corresponds to a maximum size of 10–12 mm (UNE-83607). Using this size the pumping is favoured without obstructing the nozzle and reducing the material rebound. Sandy content lower than 8 mm will not exceed 10% of total cement mixture, and the finer content will be of about 4 and 8%. The finer deficit will be compensated by means of cement and additions like silica fume. On the contrary, if the fine content exceeded these previous values more water would be added to the paste being the water-reducing additive diminished.

Accelerating admixtures

The use of shotcrete in underground rocks requires compliance with some basic requirements such as early age strength and the possibility of being applied in thick layers without the risk of displacement. The compliance with these requirements, for both dry and wet mix shotcrete, is normally achieved by using accelerating admixtures. However, despite its large application, there is not yet consensus on how to evaluate the efficiency of such admixtures /Prudêncio 1998/. For shotcrete applications the proportion of accelerating admixtures is of 3–5% with respect to cement weight (UNE 83607). Chemical compositions include some inorganic components such as soluble chlorides, carbonates, hydroxides (powder form), sodium silicates, aluminates, fluoro-silicates, and some organic components such as triethanolamine. Calcium chloride is the most common accelerator used in concrete. However, the UNE 83607-1994 norm prevents the use of any chloride type, due to problems related to steel corrosion in most environments. Hence, other chloride-free admixtures are preferred such as sulphates, formates, nitrates or triethanolamine and they have been successfully used in concrete /Prudêncio 1998/.

Triethanolamine [$N(C_2H_4OH)_3$] is an oily, water soluble liquid, produced by reaction between ammonia and ethylene oxide. Calcium formate is another type of non-chloride accelerator. At equal concentration, calcium formate [$Ca[CHOO]_2$] is less effective in accelerating the hydration of C_3S than calcium chloride and a higher dosage is required to impart the same level of acceleration as $CaCl_2$.

Set-Retarding admixtures

Retarding admixtures (retarders) delay the hydration of cement without affecting its long-term mechanical properties.

Many researchers have studied the mechanisms of set retardation and several theories have been offered to explain this mechanism. /Young 1972/ presented a review of these theories. The role of retarding admixtures could be explained in a simple way: the admixtures form a film around the cement components (by absorption), thereby preventing or slowing the reaction with water and the thickness of this film will dictate how much the rate of hydration is retarded. After a given time, this film breaks down, and normal hydration proceeds.

The main chemical compounds for set-retarding admixtures are the lignosulphate acids and the hydroxycarboxylic acids. Other important materials used in producing set retarders are sugars and their derivatives.

Fibre-Reinforced shotcrete

Non-reinforced shotcrete, like non-reinforced conventional concrete, is a brittle material that can experience cracking and displacement when subjected to tensile stresses or strains. The addition of fibres to the mixtures results in an increase of ductility as well as capability of energy absorption and impact resistance (Figure 3). The composite material is capable of sustaining post-crack loadings and often displays the increased ultimate strength, particularly tensile strength /Hoek 2000/.

Many researchers have studied the reinforced concrete degradation; however, there is not much information available about the behaviour of fibre reinforced shotcrete. In common reinforced concrete, the most habitual problem when concrete contacts saline water, is metal depassivation. It is likely that such problem may also occur in fibre-shotcrete.

Depassivation is the loss of the protective layer constituted by alkali oxides covering the metal surface. Chloride waters may dissolve the alkali oxides forming this protective layer and, therefore, may enhance steel corrosion, producing damages in the shotcrete structure.

Polypropylene fibres are in some cases used instead of steel fibres in order to avoid corrosion. Polypropylene fibres are very resistant to chemical attack and they are characterized by similar mechanical features than those of metallic fibres /Huang 2001/. The setting time is considerably reduced and they can cause a porosity increase, resulting in a drop of the compressive strength /Huang 2001/. The use of polypropylene fibres must be always implemented in presence of superplasticizers, given that they reduce significantly the porosity in the paste.

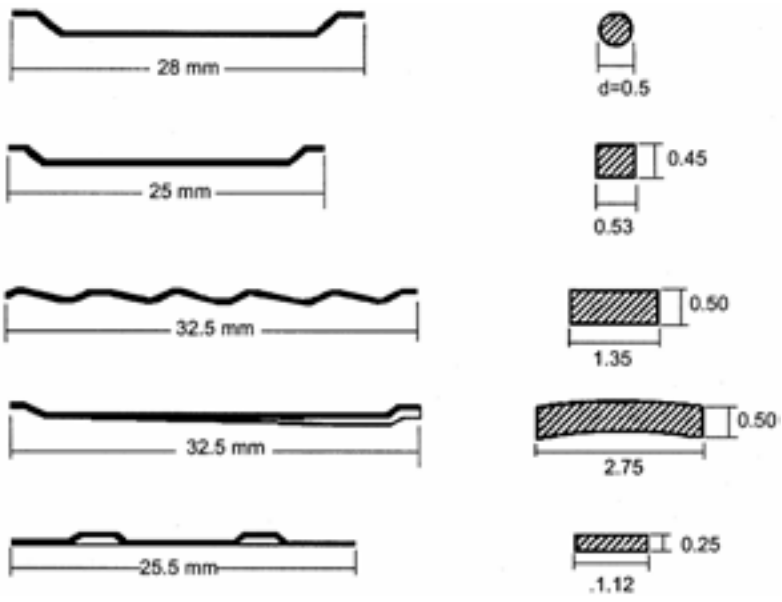

Figure 3. *Different types of steel fibres used in reinforced shotcrete applications /Hoek 2000/.*

Superplasticizers

Superplasticizers are linear polymers containing sulphonic acid groups attached to the polymer backbone at regular intervals /Mor and Mehta 1984/. These polymers have a very high molecular weight (10,000 to 100,000 times the molecular weight of water). The objective of these polymers is to produce flowing concretes with very high workability without modifying the water-cement ratio (w/c) or to maintain workability reducing this w/c ratio. The major application is the production of high strength concretes at w/c ratios ranging from 0.3 to 0.4.

In shotcrete applications, superplasticizers are necessary to obtain workability in cement pastes with a w/c ratio lower than 0.4–0.45. Doses between 3 and 5 times higher than those used for conventional concrete must be applied in shotcrete, since very fine sand and silica fume are added. In shotcrete the normal dosage of a superplasticizer ranges between 750 ml and 2,500 ml per 100 kg of cementitious material (UNE-83607).

The most common superplasticizers used in shotcrete applications belong to one of the following groups /Mor and Mehta 1994/:

- Sulphonated naphthalene-formaldehyde condensates (NS)
- Modified lignosulphonates (LS)
- Sulphonated melamine-formaldehyde condensates (MS)
- Polycarboxylate derivatives (PC)

Structural formulae of main superplasticizers are detailed in Figure 4.

The sulphonic acid groups are responsible for neutralizing the surface charges on the cement particles and causing dispersion, thus releasing the water tied up in the cement particle agglomerations and thereafter reducing the viscosity of the paste and concrete /Midness and Young 1981/. Displaced water is used to hydrate cement phases producing a large fluidity and then, a better emplacement. These effects last for approximately 2 hours.

The ability of superplasticizers to increase the workability of concrete depends on such factors as the type, dosage and time of addition of superplasticizer; w/c; and the nature of cement. The capability of superplasticizers to reduce water requirements in 12–25% without affecting the workability, leads to the production of high-strength concrete at lower permeability.

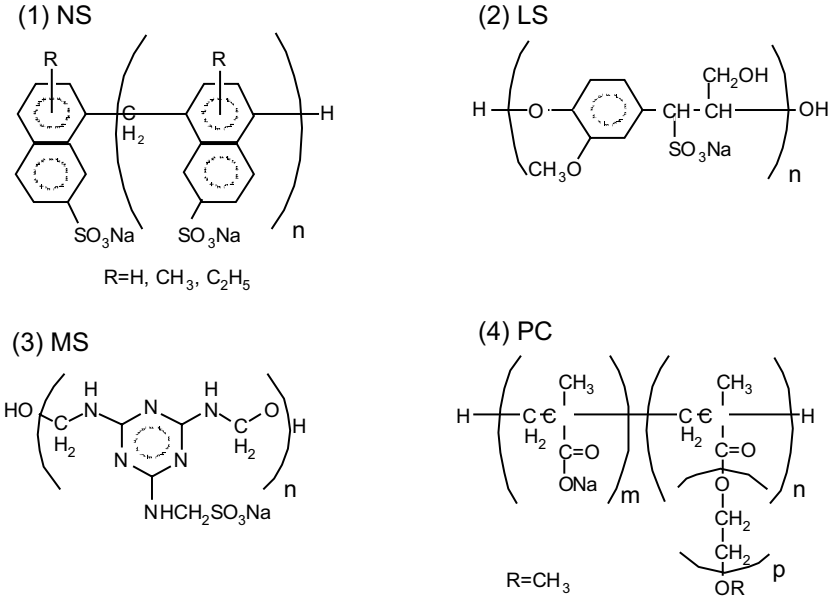

Figure 4. *Structural polymeric formulae of the most common super-plasticizers used in concrete and shotcrete.*